https://doi.org/10.5194/acp-2021-106
Preprint. Discussion started: 6 April 2021

Atmospheric Chemistry and Physics Discussions

First insights into Northern Africa high-altitude background aerosol chemical composition and source influences

Nabil Deabji[1,2], Khanneh Wadinga Fomba[1], Souad El Hajjaji[2] Abdelwahid Mellouki[3] and Hartmut Herrmann[1]

[1]Leibniz Institute for Tropospheric Research (TROPOS), Atmospheric Chemistry Department (ACD), Permoserstraße 15, 04318, Leipzig, Germany
[2]LS3MN3E-CERNE2D, Faculty of Science, Mohammed V University in Rabat, 4 Avenue Ibn Battouta, B.P. 1040, 10100 Rabat, Morocco
[3]Institut de Combustion Aérothermique Réactivité et Environnement/OSUC-CNRS, 1C Avenue de la Recherche Scientifique, 45071 Orléans Cedex 2, France

Correspondence to: Hartmut Herrmann (herrmann@tropos.de)

Abstract. Field measurements were conducted to determine aerosol chemical composition in a newly established remote high-altitude site in North Africa to investigate the variations in aerosol composition useful in assessing global and regional changes in atmospheric composition. Particulate matter (PM_{10}) filter samples (200) were collected at the Atlas Mohammed V atmospheric observatory (AM5) located in the Middle-Atlas Mountains in Morocco using a high-volume (HV) collector in a 12h sampling interval from August to December 2017. The chemical composition of the samples was analyzed for trace metals, ions, elemental carbon, organic carbon, aliphatic hydrocarbons, and polycyclic aromatic hydrocarbon (PAHs) content.

The results indicate that high-altitudes aerosol composition is influenced by both regional as well as trans-regional transport of emissions. However, local sources play an important role, especially during low wind speed periods, as observed for November and December. Despite the proximity of the site to the Sahara Desert, its influence on the atmospheric composition at this high-altitude site was mainly seasonal and accounted for only 14% of the sampling duration. Background conditions at this remote site are characterized by low wind speeds (Av. 2.5 m/s) and mass concentrations in the range of 9.8 and 20 µg/m³. The chemical composition is found to be dominated by inorganic elements, mainly suspended dust (47%) and ionic species (16%), followed by organic matter (15%), water content (12%), and indeterminate mass (9%). Biogenic organics contributed up to 7% of the organic matter with high contributions from compounds such as Nonacosane, Heptacosane, and 2-Pentadecanone. The AM5 site is dominated by four main air mass inflow, which often leads to different aerosol chemical compositions. Mineral dust influenced was seasonal and ranged between 20 and 70% of the PM mass with peaks observed during the summer and was accompanied by high concentrations of SO_4^{2-} of up to 1.3 µg/m³. During winter, PM_{10} concentrations are low (< 30 µg/m³), the influence of the desert is weaker, and the marine air masses (53%) are more dominant with a mixture of sea salt and polluted aerosol from the coastal regions (Rabat and Casablanca). During the daytime, mineral dust contribution to PM increased by about 42% because of road dust resuspension. In contrast, during night-time, an increase in the concentrations of PAHs, ketones, and anthropogenic metals such as Pb, Ni, and Cu was found due to variations in the boundary layer height. The results provide first insights into typical North African high-altitude background aerosol chemical composition useful for long-term assessment of climate and regional influence of air pollution in North Africa.

https://doi.org/10.5194/acp-2021-106
Preprint. Discussion started: 6 April 2021

Atmospheric Chemistry and Physics Discussions

1 Introduction

Aerosols are important constituents of the atmosphere due to their role in controlling climate processes and their impact on air quality, environment, and ecosystems. They can have adverse effects on human health and have been associated with respiratory disorders, strokes, pulmonary and cardiovascular diseases (Du et al., 2016; Pope et al., 2018; Song et al., 2014). Aerosol particles can serve as cloud condensation nuclei and as substrates for heterogeneous reactions (Leng et al., 2014). Their chemical composition affects aerosol-cloud interaction and may exert a warming or a cooling influence on the atmosphere due to direct and radiative forcing (King et al., 2003; Satheesh and Krishna Moorthy, 2005). Therefore, the study of aerosol chemical proprieties is essential for a better understanding of atmospheric processes.

Atmospheric aerosol particle composition depends on local and regional emission sources as well as transboundary pollution. The particles are emitted directly into the atmosphere from natural sources such as sea salt or mineral dust and anthropogenic activities such as industrial or traffic emissions, constituting primary emissions. They can also be formed in the atmosphere through gas-to-particle conversion or particle-phase reactions, constituting secondary aerosols (Carter et al., 2005). After emission, these particles are exposed to changing humidity, temperature, pressure, and solar radiation in the atmosphere that alters their properties through different aging and oxidative processes during atmospheric transport. Consequently, high-altitude sites provide the required infrastructure for investigating and characterizing the possible atmospheric aerosol interactions associated with the particles.

High-altitude sites in remote regions are less affected by direct local anthropogenic emissions. Their high altitude allows the study of aerosol particles in the free atmosphere and provides a good impression of aerosol background concentrations. The topography, meteorological conditions, and changing boundary layer heights provide various pathways for aerosol interactions, which could influence inversion processes and enhance biogenic particle formation.-Such sites are hence unique for monitoring the temporal variation in the aerosol chemical compositions over longer periods and provide a better understanding of various factors, such as meteorology, climate, and environmental changes that may in the long-term effect the local and regional air composition (Okamoto and Tanimoto, 2016).

There is increasing interest in atmospheric aerosol studies at high-altitude sites. Studies have investigated the aerosol chemical composition in mountainous regions, highlighting the influence of mountain valleys, night-time mountain breeze, and topography in dispersing polluted air masses to the free troposphere (Zhang et al., 2009; Alastuey et al., 2005; Buchunde et al., 2019; Leena et al., 2017; Glasius et al., 2018; Lugauer et al., 1998; Mukherjee et al., 2020). Furthermore, other studies at the Northeastern Himalayas, India (Chatterjee et al., 2010), the Bachelor Observatory Mountain in Oregon, USA, (Ambrose et al., 2011), a Mountain site at Lulang on the southeast Tibetan Plateau, China (Zhao et al., 2013) have reported the importance of the aerosol chemical composition at mountain sites in the identification of potential source regions of anthropogenic pollutants and their mechanism of transport. Some observation and some models have elaborated emission for some trace gases such as CO and O_3 from the boundary layer into the free troposphere by convective, frontal, and orographic lifting at mountain sites (Bey et al., 2001; Ding et al., 2015; Liang et al., 2004; Weiss-Penzias et al., 2006). Nevertheless, the effects of these mechanisms have rarely been studied at the aerosol chemical composition scale. Despite the increasing interest in high-altitude aerosol research, most studies measure tracer gases over the long term, only a

https://doi.org/10.5194/acp-2021-106
Preprint. Discussion started: 6 April 2021

Atmospheric Chemistry and Physics Discussions

few studies have focused on aerosols through short measurement campaigns, but limited studies have addressed the interaction between natural emissions such as mineral dust, biogenic compounds, and anthropogenic emissions in the free troposphere.

Moreover, such studies have been reported mostly in central Europe Asia, and North America (Okamoto and Tanimoto, 2016). A few attempts in Africa have been made to investigate the microphysical properties of mineral dust transport in North-Africa. Other studies have focused on polluted regions (Benchrif et al., 2018; Inchaouh, 2017; Tahri et al., 2013), such that information about the chemical composition of particulate matter at high-altitudes is limited. Likewise, background aerosol information, essential in assessing long-term regional changes in atmospheric composition in this region remains scarce and difficult to assess due to lack of the necessary infrastructure. This poor state of knowledge limits transregional investigation on the effect of different sources and source regions on the chemical composition of aerosol particles over sensitive regions such as the Atlas Mountains in North Africa.

The Middle-Atlas region located in the North of Morocco is typically considered as an area with high rainfall. Still, according to the report from the Moroccan ministry of environment, the annual average rainfall decreased by about 100 mm, with an increase in temperature by about 1.5 °C (Royaume du Maroc, 2009) within the past 50 years. These are indicators of the sensitive nature of the Middle-Atlas region to a changing climate. The Ifrane national park, which is located in the Middle-Atlas, suffers from intense pressure due to forest degradation, and overgrazing resulting in significant climatic consequences (Campbell et al., 2017). At the same time, it is classified as a site of biological and ecological interest. Recently, soil erosion was particularly intense in some clay-dominated valleys (Mounir et al., 2019). This change can lead to several consequences such as an increase in aridity, reduction of precipitation, change in primary emissions, and atmospheric composition. Thus, the observations from this region could provide new knowledge into atmospheric composition changes over time, related to different climatic and anthropogenic dynamics. The evaluation of local regional, trans-regional, and climate change effects can help assess air quality and climate-relevant mitigation strategies.

The aim of this study was, therefore, to i) quantify and characterize the variability of PM_{10} mass concentration in the high-altitudes of the Middle-Atlas region, ii) determine their chemical composition, iii) identify the possible sources of the aerosol particles, and iv) evaluate the relative contributions of the source regions to the observed concentrations. Within the present study, chemical composition at the high altitude AM5 observatory is presented. Chemical components such as trace metals, OC, EC, ionic, and organics species were investigated, and meteorological and back trajectory analysis was performed. Moreover, the influence of dust on the chemical composition and the day and night variation of the PM_{10} concentration were investigated.

2 Experimental

2.1 Site description and particles sampling

The Atlas Mohammed V (AM5) atmospheric research station situated in a strategic location in the Middle Atlas was founded in 2017. It is operated by the Centre National de la Recherche Scientifique (CNRS-ICARE, Orléans-France), the Mohammed V University (Rabat-Morocco), and the Leibniz Institute for Tropospheric Research (TROPOS, Leipzig-Germany). The observatory is located at Michlifen in the Middle Atlas region at an altitude of 2100 m a.s.l in a remote hilly site (33°24’22.2’’N 5°06’12.0’’W) characterized by its strategic location. On one

https://doi.org/10.5194/acp-2021-106
Preprint. Discussion started: 6 April 2021

Atmospheric Chemistry and Physics Discussions

side, the plains and plateaus of central Atlantic Morocco, on the other side, the arid areas. It is about 300 km north of the Sahara desert, about 230 km east of the Atlantic Ocean and the populated and industrial regions of Casablanca and Rabat, and about 340 km south of the Mediterranean Sea. The orientation of the Middle Atlas Mountains diagonally extends from southwest to northeast over a distance of 450 km. The AM5 station is surrounded by cedar forests and pastureland that come to life in spring and summer, which is a sharp contrast to the hot, dry climate surrounding it. The nearest urban towns are Ifrane, and Azrou, which is about 22 km away, and Fes city located 82 km north of the AM5 station. Due to its remote location, the influence of anthropogenic emissions from the Ifrane area is low.

Aerosol particles were sampled using a PM_{10} high volume Digitel (DHA-80, Switzerland) with a flow rate of 500 l/min on quartz fiber filters (Munktell, MK 360). The collection period was from August to December 2017, during which 200 filters have been collected in a day and night-time (12 h) sampling routine. At the end of the sampling, the collected filters were placed in a refrigerator at a temperature of 5°C and subsequently frozen at - 20°C. After storage, the filters were transported at -20°C to TROPOS (Leipzig-Germany) in aluminum cans for chemical analysis.

2.2 Local meteorology and station characteristics

Meteorological data were collected from summer 2017 to spring 2018 for major parameters such as temperature, relative humidity, wind speed and direction, atmospheric pressure, visibility, and precipitation at a sampling rate of 1 min using an automated weather station (Bresser AWS, Germany). As shown in Table 1, in summer, temperatures are moderate or warm during the day, cool at night. Winter is much colder, and the daily amplitudes are lower. The valleys only receive the sun's rays in the middle of the day. In winter, the station remains entirely in the shade for several weeks. Thermal contrasts between slopes are important when the topographic terrain is oriented east-west. In the valleys in high-pressure weather, thermal breezes are common. The temperature varies seasonally, especially during the transition from summer to winter, with maximum and minimum values of 26°C and -1°C, respectively. The annual average temperature is approximately 14°C, with a sharp decrease during the night.

In contrast, the visibility varies slightly, with intense UV radiation during summer when the sky is often clear. Fog occurrence is high during autumn and winter. The wind comes from all directions, but it is dominated by air mass from the west, as shown in Fig. 2. The average wind speed at AM5 was about 21 km/h but reached a maximum of 71 km/h due to turbulence in the mountain region, especially during winter. Over the summer, the minimum wind speed was about 6 km/h, and the relative humidity (RH) was low. In autumn, RH was on average about 36% and reached up to 97% under the influence of marine air mass in winter. The Middle-Atlas region is considered a very humid and temperate climate. Indeed, the water balance required for plants is mainly positive in winter, about 141 mm, while annual precipitation is 300 mm. Rainfall occurs mainly during winter, with heavy thunderstorms and a lot of snow coverage. The northern part of the Middle Atlas Mountains is the wettest region in Morocco after the Rif mountain regions, according to Nourelbait et al. (2016). Precipitation increases in frequency and intensity during the winter. Indeed, the mountain imposes an ascent of air masses, which results in

https://doi.org/10.5194/acp-2021-106
Preprint. Discussion started: 6 April 2021


Atmospheric Chemistry and Physics Discussions

cooling, the formation of clouds, and the condensation of water vapor. The proportion of snowfall also increases rapidly because of the altitude, especially in winter.

There is a wide variation in wind distribution during the summer season, and the wind comes from all directions, except the north. A predominance of southwestern winds distinguishes it. On the one hand, western winds are characterized by a high speed of up to 72 km/h. while southeast winds have a higher frequency but a lower average speed of about 6 m/s. The low wind speed from the Southeast indicates that the Saharan dust particles may reach the Middle Atlas through this transport path. Located south of the station, the high-altitude mountains of the High Atlas, which reach 4000 m in altitude, act as an obstacle or a barrier that hinders the crossing of the Saharan dust towards the North of Morocco. Their progression depends mainly on favorable weather conditions for transport, especially during the summer, the difference in temperature between day and night, humidity, and especially the scarcity of rainfall. All these factors influence the transport of large particles from the Sahara to the Middle-Atlas during the different seasons.

During the fall season, southeast winds are dominant, showing similarities to the previous summer season, with a slight increase in high wind speed frequency. On the other hand, a strong appearance of westerly winds which were often characterized by high wind speeds (stiff breeze), reaching a maximum speed of 72 km/h. During the winter months, the wind frequency comes mainly from the west and southwest, in contrast to dominated south winds in summer.

2.3 Aerosol particle chemical analysis

Particle mass

The collected filters were weighed on a microbalance with an accuracy of 10 µg (Mod. AT261 Delta Range, Mettler) after being stabilized for 72 hours at constant temperature (20±1 °C) and humidity (50±5%), before and after sampling. The difference between the weights was determined and divided by the total sampling volume to obtain the mass concentrations. After determination of the particulate matter concentration, both organic and inorganic analyses were carried out at the TROPOS laboratories.

Carbon compounds

Organic and elemental carbon were analyzed by a thermo-optical method (Sunset Laboratory Inc. U.S.A) at a maximum Temperature of 850°C with the normalized temperature program EUSAAR2 (EUropean Supersites for Atmospheric Aerosol Research), as described in the literature (Cavalli et al., 2010; Yttri et al., 2019). The method is in line with the standard proposed by the European networks (ACTRIS, EMEP). Samples were thermally desorbed from the filter medium under an inert He-atmosphere followed by an oxidizing O_2/He-atmosphere using carefully controlled heating ramps. A flame ionization detector is used to quantify methane after catalytic methanation of CO_2. First, the sample is heated up to about 870°C in an inert atmosphere of pure helium. These conditions allow the organic carbon to volatilize and to be fed into the second furnace filled with Mn_2O (oxidation catalyst), where it is quantitatively oxidized into CO_2. As a second step, the sample is placed in an oxidizing atmosphere (helium/oxygen), leading to the oxidation and volatilization of the refractory elemental carbon remaining on the filter (van Pinxteren et al., 2015). Charring processes lead to the overestimation of EC and an underestimation of OC, resulting in lower OC/EC ratios. Therefore, an optical correction was applied for charring

https://doi.org/10.5194/acp-2021-106
Preprint. Discussion started: 6 April 2021

Atmospheric Chemistry and Physics Discussions

processes. The correction value for pyrolytic carbon is obtained by measuring the transmission of the sample with a laser (wavelength 678 nm). The limit of detection for OC/EC measurement was 0.2 µg/cm^2. Organic matter (OM) was estimated based on the $f_{OM/OC}$ conversion factor, according to Turpin and Lim (2001). Organic matter was considered to be about twice the organic carbon (OM = 2.1 *OC). Since the conversion factor depends on the specific proportion of each site, the factor $f_{OM/OC}$ = 2.1 is suggested because it takes into account aged aerosols (Turpin and Lim, 2001).

Polycyclic aromatic hydrocarbons (PAHs), oxygenated polycyclic aromatic hydrocarbons (oxy-PAHs), and ketones were detected using a Curie-point pyrolyzer (JPS-350, JAI Inc., Japan) coupled with a GC-MS system (6890 N GC, 5973 inert MSD, Agilent Technologies, CA, USA) as described by Neusüss et al., (2000).

Saccharidic compounds such as mannitol, glucose, levoglucosan, and arabitol were determined using high-performance anion-exchange chromatography with pulsed amperometric detection (HPAEC-PAD) as described by Iinuma et al., 2009.

Trace metals

Trace metals were determined using the Total Reflection X-Ray Fluorescence technique (TXRF), whereby 3 spots of 8 mm in diameter each were digested in 1.125 mL HNO_3 and 0.375 HCl using the Mars 6 (CEM, Germany) microwave. 50 µL of the digested solution was deposited on previously siliconized quartz carriers, and 10 ng of Galium was added onto the sample as an internal standard. The samples were subsequently measured using an S2-PICOFOX (Bruker AXS Microanalysis GmbH, Germany) instrument. Further details of the technique and measurement procedure have been reported elsewhere (Fomba et al., 2020).

Water soluble ions

The major ionic constituents were analyzed using a standard ion chromatography technique (ICS3000, Dionex, USA) equipped with automatic eluent generation (KOH for anions and methanesulfonic acid (MSA) for cations) and a micro membrane removal unit. Ion analysis was performed for Na^+, NH_4^+, K^+, Mg^{2+}, Ca^{2+} cations, and Cl^- and Br^-, NO^-, SO_4^{2-} and $C_2O_4^{2-}$ anions. For these analyses, 3 spots of 2 cm each in diameter were extracted from the filter in deionized water via shaking for 2 h. The extract was filtered through a 0.45 µm unidirectional syringe filter to remove insoluble matter, and the filtrate was analyzed. The blank field filters were analyzed using similar procedures and were subtracted from the sample concentrations following the methodology described by Iinuma et al. (2009).

Estimation of Sea salt components

Sea salt concentrations were calculated by adding chloride to sodium, and the sea salt (ss) contributions of potassium, calcium, and sulfate where ss-K^+, ss-Ca^{2+}, ss-Mg^{2+}, and ss-SO_4^{2-} have been estimated as 0.03, 0.5, 0.12, and 0.25 fractions of the measured Na^+, respectively. The estimation of non-sea salt sulfate (nss-SO_4^{2-}) was estimated by subtracting the contribution of ss- SO_4^{2-} from the total SO_4^{2-} mass concentration (Amodio et al., 2014). The water content of the samples was estimated according to the E-AIM (Extended Aerosol Inorganics Model) III of Clegg et al. (1998).

https://doi.org/10.5194/acp-2021-106
Preprint. Discussion started: 6 April 2021

Atmospheric Chemistry and Physics Discussions

2.4 Determination of mineral dust

Mineral dust (MD) is a significant contributor to atmospheric particulate matter especially in North-Africa, where the average percentage can vary from 7% to 62% (Gherboudj et al., 2017). The high spatiotemporal variability of the dust emission can sometimes be difficult to quantify correctly and may lead to some uncertainty. Therefore, the estimation of MD can be subjective because several estimation methods are available in the literature. The most common methods were applied to the samples collected at AM5 station. Within the present study, the aim was first to evaluate and then select an appropriate method for the interpretation of the results. Four methods were highlighted that are representative of those used in the literature. The first method implemented by Fomba et al., (2014) consists of subtracting the total PM_{10} mass concentration from the analyzed mass of the other elements, representing the upper limit of the possible MD concentration in the samples. This method is an interesting approach especially when the elemental analysis is not available. However, to improve on the MD quantification using available MD-related elements, applying a stoichiometric equation reduces the uncertainty of the values. Using this method, an average MD concentration of about 24.5 µg/m^3 was obtained. In contrast, methods 2 and 3 use different approaches. They estimate MD base on given stoichiometry and apply different elemental concentrations such as Al or Ca, Fe, Ti to estimate the MD load. Method 2 use the factor (1.16) to compensate the exclusion of MgO, Na_2O, K_2O and H_2O fron the crustal mass calculation, as shown in Table 2 (Maenhaut et al., 2005). Whereas method 3 considers carbonate such as calcite, dolomite and other oxides such as TiO_2, Fe_2O_3, and MnO_2 (Minguillón et al., 2007; Nerriere et al., 2007). As a result, the average MD concentration using methods 2 and 3 were similar, about 19.9 and 18.9 µg/m^3, respectively. Method 4 takes into account that sea salt significantly affects these concentrations, and the non-sea salt (nss) content of the elements, such as nss-Ca^{2+} or nss-Mg^{2+} are used to replace the total Ca and Mg concentrations. This is more accurate in a sea-salt-dominated environment but could underestimate the calcium contribution as sodium also has a crustal origin (Cesari et al., 2012; Perrino et al., 2014). The MD concentration from this method was about 15.5 µg/m^3.

In conclusion, differences of up to 37% were obtained between these methods. The obtained MD concentrations were high for method 1 and lowest for method 4 and similar between methods 3 and 4, indicating their robustness. Thus, this approach was applied in this study to estimate the MD content. Method 3 does not consider quantifying silicates SiO_2 and aluminosilicate Al_2 SiO_2, a major component in natural mineral dust. While method 2 allows to take into account the overall mineral composition and therefore was applied in this study. Due to limitation in quantifying Si from quartz fiber, MD was finally estimated by replacing "Si" with "Ca" base on the established soil stoichiometric ratio of the average upper continental crust (Si=10.3 Ca), according to Wedepohl (1995) in the equation used in Method 2. The final equation used for mineral dust estimation is given as follows:

$$\boldsymbol{Mineral\ dust} = 1.16(1.90\ Al + 23.3\ Ca\ + 2.09\ Fe + 1.67\ Ti), \quad (1)$$

2.5 Back trajectory analysis

Air mass back trajectory analyses were performed to assist in the data interpretation of the data. A PC version of the NOAA HYSPLIT (Hybrid Single-Particle Lagrangian Trajectory) model was used to calculate 96 h back trajectories for every hour within the sample collection interval. Ensembles of the back trajectories were obtained as described in van Pinxteren et al., (2010). Meteorological input data from the GDAS database were obtained from the NOAA HYSPLIT website. Vertical velocity fields (default HYSPLIT option) were included with

https://doi.org/10.5194/acp-2021-106
Preprint. Discussion started: 6 April 2021


Atmospheric Chemistry and Physics Discussions

meteorological data. The model was run in ensemble mode with a starting height of 2000 m above ground level. Air masses reaching the site were characterized by 96h back trajectories (every 3h) using the computer HYSPLIT version (Draxler, 2003) at an altitude of 2000 m and coupled with the GDAS (1°) meteorological database (Stein et al., 2015). The trajectory ensemble is made up of several trajectories determined for the same spot. The classification process using backward trajectories determines the percentage of air mass for each sample after identifying the potential air mass. Meteorological data, including wind direction and speed, were used to allow additional regional accuracy. The main goal was to determine the most prevalent air mass per sample.

3 Results and discussion

3.1 Variation of PM_{10} mass

3.1.1 Daily & monthly variation

The PM_{10} mass concentration time series at the AM5 station shows a strong temporal variation, with an average of 29.2 ± 17.3 µg/m^3 as illustrated in Fig. 3a. During the five months of measurement from August to December 2017, particulate matter mass varied from 9.5 µg/m^3 to 145.6 µg/m^3. The monthly variation of PM_{10} mass concentration indicates a monotonously decreasing trend with an average of 49.9 ± 25.9 µg/m^3 during August, and 16.1 ± 5.6 µg/m^3 in December. In September due to power failure and instrument outage fewer samples were collected (n=20) and the average PM_{10} mass was 26.64 ± 5.2 µg/m^3. Due to the lower number of samples, the September average is not further discussed in detail. The average PM_{10} mass in October and November was about 30.5 ± 10.7 and 22.8 ± 7.9 µg/m^3, respectively.

The observed temporal variation in the concentration is related to factors such as meteorological conditions and the air mass arriving at the station – accordingly the high particle mass concentration observed during August was due to the influence of Saharan dust events. During such events, PM_{10} mass concentration reached up to 143 µg/m³ and often exceeded 80 µg/m^3. The meteorological conditions at the Atlas Mountain shown in Table 1 highlight the low humidity and often low precipitation during the summer period. These specific conditions favor the transport of dust particles from the Saharan desert to the high-Atlas Mountains.

In contrast to the summer period, PM_{10} mass concentration was low during October, November, and December, despite some episodic anthropogenic influences. The particle mass concentrations decreased because of higher precipitation during this period. The mentioned months had many days with typical background baseline conditions with low PM_{10} mass concentrations at the AM5 station, as shown in Fig. 3a. The days with low concentration were typically days with low wind speed and days directly after precipitation events. These days typically occur in the Autumn when the precipitation frequency was higher than in August. The relative humidity, , as indicated in Table 1. also increased with maximum values up to 92%.The typical background PM_{10} mass concentration at the Atlas ranged between 9.8 and 20 µg/m^3, which were observed to be stable and representative during periods of little external influence. The high PM_{10} concentration of up to 145 µg/m^3 was recorded during periods of air mass influence from the Southeast especially during August (Fig. 3b). This further indicates that the potential source of the particles is the Saharan desert, as suggested previously. The distribution of PM_{10} concentration appears homogeneous with a slight influence of West winds. The average PM_{10} concentrations were

https://doi.org/10.5194/acp-2021-106
Preprint. Discussion started: 6 April 2021


Atmospheric Chemistry and Physics Discussions

in the range of 20 to 40 µg/m^3, despite the occurrence of southerly winds. In winter, there is a change in the wind direction from south to west which leads to a decrease in the PM_{10} concentration. The average concentration when the wind was from the west was 15 µg/m^3. During winter, there is also an increase in precipitation, which could leads to a drop in concentration due to the particle washout effect. Therefore, despite the high wind speed from the west and southwest, the PM_{10} concentration was not significantly affected.

3.1.2 Comparison with other stations

PM_{10} concentrations at AM5 were compared with those of similar high-altitude as well as Urban and marine sites. High-altitude sites with available PM10 concentrations in tropical regions, as well as regional studies in Urban and marine regions were compared. Table 3 presents the PM_{10} mass concentration of the different sites, the site types, the reported data period, site altitude, and the corresponding references.

AM5 PM_{10} concentrations are comparable to concentrations reported in other high-altitude regions such as in Mahabaleshwar (India), Lhasa (Tibet), Sinhagad (India), or Darjeeling (India). The AM5 station shows a similarity with the Darjeeling station (West Bengal, India) situated at the base of the Himalayas. The two stations are approximately similar in altitude (2000 m) and have comparable average PM_{10} mass concentrations (29 µg/m^3). According to Table 3, the concentration of particulate matter varies with altitude but also dependent on the prevalent local and regional emissions, sampling period, as well as meteorology around the site. The high-altitude sites often experience changing atmospheric as well as convective boundary layer heights that affect their aerosol concentrations (Coen et al. 2018).

The observatory of Izaña, which is located near the Moroccan Atlantic coast, has a 6 years average concentration of about 46.2 µg/m^3. The high concentration was mainly due to the transport of Saharan dust from the African continent occurring in summer and episodically in spring (Rodrıguez et al., 2009). A slight difference was observed in PM_{10} mass with the other high-altitude stations in Tibet and India. In comparison to the AM5, the concentrations there were higher at about 37.7 and 35.8 µg/m^3 due to high-dust load and the proximity of the stations to urban activities (Zhao et al., 2013). PM_{10} concentrations at AM5 were comparatively lower than those reported at Kathmandu, Nepal, which is almost at the same altitude as the site. In contrast, the high concentrations recorded in Kathmandu of about 169 µg/m^3 were mainly due to the resuspension of road dust or ash from local combustion sources due to the proximity of the site to urban cities (Putero et al., 2015). The influence of desert dust transport to the Himalayas resulted in high coarse mode aerosol particles in the Northeastern region (Chatterjee et al., 2010). The comparison with the Cape Verde marine station shows a larger difference which has an average mass concentration of about 47.2 µg/m^3. The influence of marine emissions due to its proximity to the ocean and dust transport from the Sahara to the American continent explains the high concentrations recorded at this site. In contrast, the background marine station in the Mediterranean has a lower average PM_{10} mass concentration of approximately 18.2 µg/m^3 despite the occasional influence of natural aerosols particle emissions including Sahara dust and marine aerosol, which contributes about 39% of the total PM_{10} mass (Scerri et al., 2016).

The observed PM_{10} mass concentrations at AM5 were compared with those reported from other sites in Morocco (Table 3). The comparison with the urban sites shows a large discrepancy with higher values of about twice or trice those observed in the Middle Atlas region. The concentration of the North-African urban cities varied on

https://doi.org/10.5194/acp-2021-106
Preprint. Discussion started: 6 April 2021

average between 31 µg/m^3 and 80 µg/m^3, depending on the characteristics of each city. Marrakech and Tunis have similar concentrations of 52 µg/m^3 and 58 µg/m^3, respectively, due to the high traffic and combustion emissions (Kchih et al., 2015; Inchaouh, 2017). Agadir has more pollution (65 µg/m^3) due to higher industrial emissions and the influence of sea salt due to its location along the Atlantic coast (Ajdour et al., 2019). Tetouan, which is located in the north of Morocco on the Mediterranean coast, has a low concentration. Tinfou, a station located in the Sahara, has a high concentration due to its proximity to the source of natural dust emission (Knippertz et al., 2007; Tahiri et al., 2016). The urban concentration of Moroccan cities remains low compared to Delhi in India, for example, which has a concentration of about 232 µg/m^3. In conclusion, the PM_{10} mass concertation at the AM5 indicates its characteristic as a high-altitude remote station located in a rural area as those observed in other regions in the world.

3.2 Aerosol composition under remote background conditions

3.2.1 Background conditions at the remote site

The term 'background conditions' has diverging interpretations in the literature. It defines the composition of aerosol particles necessary to establish a baseline to identify sources of pollution and to quantify the contribution of the pollutants (Council et al., 2010). Calvert (1990) defines background concentrations as the concentration of a given species in an air mass considered to be clean, in which anthropogenic impurities are not contained. However, the continuous variation of an air mass and a possible anthropogenic influence during long-range transport could influence this condition. Parrish et al., (2012) thus prefer to use baseline conditions and not background conditions and refer it to measurements obtained when local emissions are considered to be negligible.

Background conditions are considered in this study as periods where long-range transport and extreme weather and external influences are low, which is representative of a typical regional atmosphere. A few criteria were applied to select the samples that are representative and typical of such background conditions in this remote region. They were periods when the particulate matter mass concentrations were lower than 20 µg/m^3 and low wind speeds less than 4 m/s. Samples considered to be mainly influenced by local anthropogenic pollution or Saharan dust event were not taken into account. The samples obtained when air mass came from the Atlantic Ocean without passing through coastal urban and industrial regions are a typical air mass inflow during remote background conditions. The air mass coming from the Mediterranean Sea also met the criteria established for the selection of background condition samples. After applying the selection criteria, a total of 60 samples were representative of remote background conditions.

3.2.2 Background chemical composition

In the following, the characteristics of the particles that were observed during background conditions will be elaborated on and their variations discussed. The statistics of the quantified chemical species, including their mass concentrations, min, max, and standard deviations are provided in Table 4.

https://doi.org/10.5194/acp-2021-106
Preprint. Discussion started: 6 April 2021

Atmospheric Chemistry and Physics Discussions

Relative composition

The average PM_{10} mass concentration during background conditions was 15.2 ± 5.9 µg/m^3 while the average pH of the particles was about 5.9 indicating that the particles during these conditions were acidic. Figure 4 shows the average relative composition of the major chemical species for PM_{10} observed at the AM5 site during background conditions. This aerosol particle composition is dominated by mineral dust (47%) and organic matter (15%). Aerosol water content accounts for 12% due to high humidity in Atlas mountain regions, as mentioned previously in Table 1. According to Kreidenweis et al. (2008), atmospheric aerosol can contain up to 30% of water at 50% relative humidity, which is similar to the observed results. Inorganic ions, including sulfates, nitrates, and ammonium, made up 6%, 5%, and 3%, respectively. Sea salt and elemental carbon account for about 2% and 1% of the PM10 mass, respectively.

Inorganic species

Since mineral dust dominates the chemical composition of the particulate matter, metals such as Al, Fe, Ca, Ti, or Mn, which are considered as good tracers of mineral dust, showed comparatively high average concentrations in comparison to other elements. The composition of the local mineral dust is characterized by a clear dominance of Ca (ca. 874 ng m^{-3}) due to the major presence of calcium-rich minerals such as gypsum, dolomite, and calcite in the soil composing the Middle Atlas (Khrissi et al., 2018; Miche et al., 2018). The AM5 site is not permanently influenced by mineral dust from the Sahara, as the mineral dust in the background condition reflects the geological composition around the site and the resuspension of road dust as shown by the Fe/Ca (≈0.92) and Fe/Al (≈0.98) ratios. Heavy metals such as Cr, Cu, and Pb were relatively low, except Zn, which reaches a concentration of 43.5 ng m^{-3} with an average of 21.6 ng m^{-3} during the remote background conditions. Its correlation with other metals of crystalline origin indicates that it is sourced from the erosion of Zn-containing soil particles (Noulas et al., 2018). Also, elemental carbon (EC), which is considered as a good tracer of anthropogenic pollution, remains low on average 0.25 µg/m^3, except for a few days that it reached 0.75 µg/m^3, which indicates the low local anthropogenic influence probably nearby car exhaust emissions during remote background conditions.

The secondary inorganic aerosol that contributed 11% of the PM_{10} total mass showed that compounds such as NO_3^- (0.81 µg/m³) and SO_4^{2-} (0.89 µg/m³) were high in comparison to NH_4^+(0.29 µg/m^3). This enhanced anion concentration is also reflected in the low aerosol pH value observed during this period. Other cations of mineral origin, such as Na^+, K^+, and Mg^{2+}, have lower concentrations in comparison to Ca^{2+}, of about 0.21, 0.04, and 0.06 µg/m^3, respectively, as a result of the resuspension of soil. The concentration of Cl^- remains low, at about 0.07 µg/m^3. Na also showed a correlation with other mineral elements such as K and Mg, indicating it could also have, in addition to sea salt, crustal matter origin.

Organics

Organic compounds, including aliphatic hydrocarbons, polycyclic aromatic hydrocarbons (PAHs), and ketones were also detected in background samples, as presented in Fig. 4b, 4c and 4d. In total, 11 n-alkanes, 7 PAHs, and 5 ketones were detected during background conditions in the Atlas mountain regions accounting for 7% of the total organic matter. The average background concentration for n-alkanes, PAHs, and ketones were 0.72 ± 0.41 µg/m^3, 0.12 ± 0.28 µg/m^3, and 0.92 ± 0.25 µg/m^3, respectively. Aliphatic hydrocarbons were mainly natural source biogenic emissions that could account for the high abundance of alkanes such as Hentriacontane, Nonacosane, Heptacosane, which made up 21%, 19%, and 11% of the total alkanes, respectively. Significantly higher

https://doi.org/10.5194/acp-2021-106
Preprint. Discussion started: 6 April 2021


Atmospheric Chemistry and Physics Discussions

concentrations of odd-numbered n-alkanes were found in background conditions samples, especially C_{23}, C_{25}, C_{27}, C_{29}, and C_{31}, which implies that these species are from terrestrial plants (Waples, 1985). Besides, alkanes with a high molecular weight were predominant. The carbon preference index (CPI) was calculated according to the CPI formula proposed by Marzi et al., (1993). The CPI was on average 1.14, which indicates that input from biogenic compounds emitted from the local vegetation was mainly dominant. During this period, PAHs were strongly dominant with up to 81% by fluorene, a tracer of the combustion of gasoline or diesel fuel. Fluorene is naturally present in tar, more precisely in the high-boiling fractions, indicating that it originates from the roads around the site. Major ketone constituents were 2-Heptadecanone, 2-Nonadecanone, and 2-Pentedecanone, which represent 33%, 26%, and 22%, respectively. These organic compounds that appear in fossil fuel burning events were found in low concentrations at the AM5. The organic material composition during background conditions shows a variety of plant and microbiological activity surrounding the station. It also provides information on local pollution state, which is considered negligible.

Besides mineral dust, organic matter (OM) also constitutes a high fraction of the background PM_{10}, with an average concentration of 1.12 µg/m^3, and a maximum of 4.5 µg/m^3. Trace species of the organic matter were also identified. Sugar alcohols such as Mannitol, Arabitol, and Glucose, highlight the fact that some of the organic material is of biogenic origin. The contribution of sugar alcohols was significantly higher during the summer, linked to more developed vegetation and a higher biogenic activity during the hottest and sunniest months of the year as also observed at rural sites in France (Golly et al., 2019).

3.3 Air mass classification

The processing of the wind data, including speed and direction, allowed the identification of local sources at the station. This analysis was complemented by trajectory calculations using the Hysplit model. The backward trajectory analysis was used to identify the air masses arriving at the station to provide a more extensive global view. The lifetime of a particle depends on several parameters, micron-sized particles have a lifetime of 3 to 5 days (Jaenicke, 1978). By combining wind data and trajectory calculations, it is possible to determine the different sources of aerosol. This can be extremely important in the interpretation of the data. Several observed events can be explained by this combination. Air mass back trajectory were performed for all collected samples to identify the main sources affecting aerosol composition. The air mass origins were classified into four major categories, as showed in Fig.5. Given the location of the station in the Middle Atlas and the proximity of the Atlantic Ocean coasts, back trajectory analysis confirmed the dominance of the westerly air mass from the North Atlantic Ocean (NAO), which represented 53% of all samples analyzed. This air mass was, however, characterized by low PM_{10} mass concentrations on averagely 19.5 µg/m^3 as shown in Table 5. Its chemical composition is dominated by local dust 45% and organic matter 6%. Sulfate and nitrate represent only 3 and 4%, respectively. NOA is distinguished by a strong marine influence, as shown by the contribution of sea salt about 3%. In about 7 % of the cases the Atlantic air mass crossed the coast of Europe (ACE), located about 426 km north. Strong differences regarding the chemical composition can be highlighted. ACE was often associated with anthropogenic pollution, as shown by the PM_{10} mass, approximately 30.1 µg/m^3. However, the increase of sulfate and nitrate concentrations indicates that this air mass has crossed over urban cities on the coast. The concentration of sea salt and EC remains were about 2% higher than with the other air masses.

https://doi.org/10.5194/acp-2021-106
Preprint. Discussion started: 6 April 2021


Atmospheric Chemistry and Physics Discussions

The AM5 station is about 339 km south of the Mediterranean Sea. The influence of the Mediterranean Coast and Europe (MCE) was higher (about 26%) in comparison to the ACE airmass. Due to the absence of an industrial zone in the North-East of Morocco, combined with the low wind speed discussed previously, PM_{10} mass obtained at the AM5 station during the MCE influence was low, ca. 23.8 µg/m^3, as shown in Table 5. This low PM_{10} mass concentration indicates a cleaner air mass in comparison to the other air mass inflow such as ACE or Saharan Dust (SD). Mediterranean Sea air mass presents similar averaged compositions to the NOA, with a major contribution of local dust 44% followed by OM 8%. Except for the secondary inorganic aerosols such as nitrate and sulfate that have higher concentrations accounting for about 4% of the total mass. The contribution of EC and sea salt remains extremely low due to the low wind speed during particle transport to the AM5 site.

During a Sahara dust event from the 10th to the 13th of August, the mineral dust made up to 81% of the total mass, followed by organic matter with 7%. The influence of urban pollution remains very limited during Saharan air mass inflow, as shown by the low contribution of EC. The water content was low due to the transport of the mineral dust during the summer, a season characterized by the low relative humidity of about 36%, as indicated above in Table 1. Despite the proximity of AM5 to the Sahara Desert, which is located approximately 383 km in the South and East of the AM5, the frequency of the Saharan desert (SD) air mass remained low at only about 14% of the collected samples. This indicates that the transport of mineral dust particles is conditioned by the westward passage of the air mass along the Middle Atlas Mountains, which makes it possible to bypass the high-altitude mountains to the south of the station. The altitude of the high-Atlas Mountains (4000 m) prevents desert transport in the southern sector. The influence of dust on the PM_{10} mass was high at about 54.2 µg/m^3, as shown in Table 5. Back trajectories confirm the hypotheses addressed by the local wind data and indicate that the high concentration observed during August is due to the dust event.

3.4 Characterization of aerosol chemical composition for the complete measurement period

3.4.1 Mineral dust

The temporal variation of the main chemical species is shown in Fig. 6. Mineral dust is often found in all air masses, between 20 to 40% of the total mass. Most dust events occurred during the summer, as shown by the sharp increase of Fe and Al concentrations, which are considered as good dust tracers (Arimoto et al., 2006) during the Saharan dust event from 10th to the 13th of August. Mineral dust, which is present on average at a concentration of 6.3 µg/m^3 during remote background conditions, was found to be more than 10 times higher (88 µg/m^3) during dust events Other less intense Saharan dust storms occurred during the summer season between the 21st and 24th of August with a similar impact (5 times higher dust concentrations as background conditions). The Saharan dust air masses were not significantly influenced by urban pollution, as shown by the low concentrations of EC (0.2 µg/m^3) associated with their period of influence at the AM5 site. According to the back trajectories, the transport of mineral dust takes place directly from the Sahara desert situated in the south of the AM5 site, without passing through cities with intense anthropogenic activities. On the other hand, a slight increase in organic matter was observed during the dust event, as shown in Fig. 6. During this period, a correlation was observed between organic matter (as well as some organic species Nonacosane and Heptacosane) with mineral elements such as calcium (R^2=0.81) and magnesium (R^2=0.73). During the winter, this relationship became practically insignificant

https://doi.org/10.5194/acp-2021-106
Preprint. Discussion started: 6 April 2021


Atmospheric Chemistry and Physics Discussions

(R^2=0.15). Therefore, it indicates that mineral dust loaded with biogenic matter could have been observed during dust transport.

3.4.2 OM and EC

Organic matter (OM) and elemental carbon (EC) show a distinct seasonal variation with an average of 2.1 µg/m^3 and 0.3 µg/m^3. A high concentration marks the trend of organic matter during the summer, with an average of 4.4 µg/m^3 and a maximum of 70 µg/m^3. During summer, a correlation was found between organic matter, magnesium, and oxalates, which is considered a good tracer for biological activity. A correlation was also found between OM and other species from natural sources such as n-alkanes, glucose, mannitol, or arabitol, indicating that the organic matter was mainly from biogenic sources. The concentration of organics progressively decreases until the winter, where the lowest concentration was recorded, reaching an average of 1.61 µg/m^3. In the same periods, an increase of PAHs and ketones were noticed. However, the maximum concentration was observed during October of about 0.76 µg/m^3 due to long-range pollution transport. In contrast to organic matter, EC shows little temporal variation. Few pollution episodes could be observed during the sampling period, as observed by the peaks in the EC concentration in Fig. 6. The summer period was marked by low EC concentrations, with an average of 0.24 µg/m^3. On the one hand, mineral dust transport was often not influenced by anthropogenic, as shown by the unchanging elemental carbon concentration EC concentrations.

The dust deposited in the Middle-Atlas has often been loaded with biogenic material surrounding the Middle-Atlas region. The sudden increase in EC often came from two sources. Firstly, from Europe through the Atlantic Coast during ACE long-range transport air mass influence and secondly, from nearby urban regions especially in the evening when the temperature is low (with an average of 5°C)and high values of anthropogenic metals observed. The urban cities of Fes and Meknes, located about 85 and 50 km in the North from the station, are the most likely sources of pollution. Conversely, the EC/OC ratio tends to increase from summer 0.12 to 0.52 during winter. First, due to the formation of secondary organic aerosols in summer by photochemical processes, and second due to changes in the meteorological conditions, which are very unfavorable, to prevent the dispersion of pollutants (Chu et al., 2005) and third due to increased wood combustion during colder periods.

3.4.3 Sea salt

The Middle Atlas region is influenced by two maritime sources of sea salt, more often from the Atlantic Ocean, and sometimes from the Mediterranean Sea. The highest concentrations were recorded during August and September when sea salt concentrations reached a maximum of 3.4 µg/m^3. The sea salt then decreases gradually, reaching a minimum concentration of 0.06 µg/m^3 during December. The average sea salt concentrations remain low, with an average of 0.43 ±0.3 µg/m^3. Sodium has mainly two sources at AM5, a significant source from the ocean but also the crust. To differentiate between these significant sources, sodium from marine sources was estimated after the subtraction of the estimated soil sodium from the measured sodium concentration. The soil sodium was estimated using the Na/Ti ratio, according to Wedepohl, (1995). The soil originated from sodium accounted for 65% from the total concentration. The sea salt concentration was high when wind speed exceeded 6 m/s, indicating that sea salt was strongly dependent on the meteorological conditions and air mass sources. The highest contribution of sea salt to PM_{10} mass, about 11 %, was measured when the air mass came from the North Atlantic Ocean (NAO), compared to less than 1 % of the PM_{10} mass when the air masses were from the Sahara

https://doi.org/10.5194/acp-2021-106
Preprint. Discussion started: 6 April 2021


Atmospheric Chemistry and Physics Discussions

Desert (SD). As a result, sea salt was mainly present as aged sea salt. Sodium concentration was high during a pollution episode on the 16th of August. During this period, a high concentration of other elements such as EC, SO_2^{2-}, NO_3^-, and NH_4^+ was observed. This was due to the influence of ACE air masses with high EC content that made up about 5% of the PM_{10} mass at the AM5 site.

3.4.4 Ammonium, nitrate, and sulfate

The temporal variation during the sampling period of sulfate, nitrate, and ammonium is presented in Fig. 6, with average concentrations of 0.94, 0.86, and 0.29 µg/m^3, observed, respectively. In summer, the concentrations were relatively high during the first few days in August. Due to the transport of polluted ACE air masses through the coast of Europe, leading to the observation of the highest sulfate, nitrate, and ammonium concentrations with maximum concentrations of up to 6.1, 4.4, and 1.2 µg/m^3, respectively. Sulfate formation via photo-oxidation during the summer was relatively low, as no significant variations in its concentration were observed between day and night. On the other hand, long-range transport seems to have been the main origin of the observed SO_4^{2-}. Indeed, the concentration of sulfate varied from 0.66 to 7.2 µg/m^3. The ammonium sulfate trend was predominant during the summer. The highest ammonium concentration of 1.2 µg/m^3 was found during summer, however, the high concentrations were not only recorded during summer but also in the subsequent months. These were often due to ACE /MCE and NOA air mass influences at the site during which, concentrations of ammonium were found to be 2-5 times higher than during the background remote conditions.

3.4.5 Crustal enrichment factor

Trace metals are naturally present in the atmosphere originating from industrial, traffic, combustion as well as natural source emissions. Analysis of the crustal enrichment factor (EF) has been used to estimate the contributions of crustal matter to the ambient PM_{10} particles at AM5. For this study, Ti is used as a tracer for mineral dust due to the low recovery of Al and high recovery of Ti and as it is also considered a suitable tracer for mineral dust (Fomba et al. 2013). Furthermore, Al or Fe has more anthropogenic sources than Ti. However, the EF trend was similar when Al was used as a reference element, with only slight differences observed in the absolute values. The average upper continental crust composition, according to Wedepohl (1995) was used for the calculation of the enrichment factors. The EF relative to Ti is given as:

$$EF = \frac{\left(\frac{Z}{Ti}\right)sample}{\left(\frac{Z}{Ti}\right)Crust} \quad (2)$$

The enrichment factor provides the ability to classify metals based on their enrichment to the soil. Elements with an EF under 2 are considered to have a similar composition to the reference soil values. An enrichment factor above 2 but below 10 is assumed to be low enrichment with a possible mixture of both crustal and non-crustal sources. Elements with an EF above 10 are considered enriched, while enrichment factors above 100 are considered highly enriched, suggesting that the elements are from non-crustal and more likely anthropogenic sources. The enrichment factor does not take into account each pollution episode but is a general approach to the classification of metals according to their crustal origin. Within the present study, the elemental enrichment factors showed similar trends for the different air mass inflow to the station. Three groups of elements could be identified from the elemental enrichment factors.

https://doi.org/10.5194/acp-2021-106
Preprint. Discussion started: 6 April 2021


Atmospheric Chemistry and Physics Discussions

Group I includes elements such as Al, Ba, Rb, K, and Fe with enrichment factors between 0.8 and 2. Their enrichment factors suggest that these elements are associated with particulate matter from the resuspension of soil or other crustal sources. Elements such as Al, Fe, and Mn show little dispersion, and their variation seems to be constant across different air masses, clearly indicating that the source was soil. As suggested by other studies, these metals could also have an anthropogenic source, but in this study, they clearly showed crustal matter origin (Viana et al., 2008; Birmili et al., 2006; Contini et al., 2012). No correlation was found between Al, Fe, and anthropogenic tracers such as EC or other heavy metals. On the other hand, K showed slightly higher EFs for air masses from the Atlantic Ocean, suggesting that sea salt and sources other than mineral dust, such as biomass combustion, might have contributed to its presence. Indeed, the Fe/Ca ratio can be used to distinguish between potential sources of Sahara dust in northern Africa, as suggested by Formenti et al.,(2014). Fe/Ca ratios close to 0.4 indicate that the dust comes from the south, while Fe/Ca ratios higher than 1 indicate that the dust comes from the East. The average Fe/Ca ratio obtained at the station was 0.54, which suggests that the dust often originated from south Morocco. During the dust event, the Fe/Ca ratio increases to 2.52, which suggests that long-distance transport of the dust from the eastern Saharan regions was observed, which is in agreement with the pollution rose, which indicated high concentrations from southeast winds.

Group II elements include heavy metals such as Sr, Ca, Cu, Mn, Ce, V, La, Co, and As. These elements had enrichment factors ranging from 2 to 10, indicating the possibility of having mixed origin from both crustal and anthropogenic sources. In the case of North Atlantic (NOA) marine air masses suggesting that the elements may have been of crustal origin, the lowest enrichment factors were observed. In contrast, the highest enrichment factors were mainly observed in air masses that originated from the coast of Europe (ACE) and crossed major urban cities such as Rabat/Salé/Kenitra and Casablanca before arriving at Atlas station M5. In this case, it is assumed that these elements were probably influenced during transport by anthropogenic emissions. In contrast, the Mediterranean Sea air mass appears to remain relatively unaffected by anthropogenic emissions. In addition to its atmospheric crustal origin, V had a high enrichment factor mainly due to residual oil combustion, especially at night. Particles from oil combustion processes were often observed in high concentrations during winter due to their size and long lifetime in the atmosphere and the combustion activities in the nearby urban cities.

Group III contains the elements with EF from 10 to 1000, including heavy metals such as Cr, Zn, Ni, Pb, as well as Br, Se, and Sb. These elements showed high enrichment factors in all air mass directions. They are mainly present in the marine air masses of the Atlantic, but also the Mediterranean air masses. An increase in heavy metal concentration has been observed during winter, and at night when the temperature drops, the air mass inflow from the cities towards the mountain prevails. Atmospheric Ni and Cr are released during combustion processes, while Pb is mainly released from smelters or the combustion of unleaded petrol, waste, and coal (Pacyna et al., 2007). Combustion processes are generally the main contributors to these anthropogenic metals. Zn had a weak correlation with Pb and Ni, suggesting that its origin is also anthropogenic. The nearest urban cities are Meknes and Fes, where anthropogenic activities such as waste incineration, and road traffic pollution are common.

https://doi.org/10.5194/acp-2021-106
Preprint. Discussion started: 6 April 2021

Atmospheric Chemistry and Physics Discussions

3.4.6 Organic compounds

The identification of the organic chemical compounds enables a better understanding of the organic fraction in the composition of aerosols and the quantification of the contribution of biogenic and anthropogenic emissions (Jaenicke, 2005). Therefore, a large number of individual organic chemical compounds were analyzed. Figure 8 shows the temporal variation of organic compounds, including alkanes, PAHs, and ketones. Individual n-alkanes with C-atom numbers in the range 20-34 were analyzed. The distinguishing aspect of alkanes is their specific source and their ability to provide information about their origins (Pietrogrande et al., 2010). Figure 8 shows the temporal variation of n-alkanes, the background composition, which is not necessarily constant over the seasons at about 6.17 ng/m^3. In contrast, the variation of the average concentration under the influence of air masses decreases from summer (16.48 ng/m^3) to winter (4.87 ng/m^3). To distinguish between natural biogenic emissions from plants and incomplete combustion, the carbon preference index (CPI) was also calculated and used as a marker (Alves et al., 2012; Pietrogrande et al., 2011). The part of n-alkanes with an odd number of C-atoms exceeding the distribution of the average concentration of n-alkanes can be considered as coming from vegetable waxes. However, odd C-atom-numbers can also originate from incomplete biomass combustion (Iinuma et al., 2007). The concentration of alkanes is dominated by odd C-atoms with a concentration of 6.4 ng/m^3, compared to 1.9 ng/m^3 of even C-atoms. Higher concentrations were observed during the summer, approximately 39.2 and 10.4 ng/m^3 for n-alkanes with odd and even C-atoms, respectively, due to the strong biogenic activation during this season. In contrast, a low concentration was recorded during winter, around 0.11 ng/m^3. A strong correlation (R^2=0.77) was found between OC and alkanes for all samples. It is important to note that the concentration of alkanes increased by 44% compared to the background composition during summer.

In this study, 32 PAH with 3 to 7 rings were quantified. In Fig. 8 the temporal variation in the form of the sum of PAH identified in the particles is presented. The mean concentration of PAHs was about 6.9 ng/m^3. The highest amount of PAH was detected during autumn, approximately 3.1 ng/m^3. The minimum concentration was observed during winter, of about 0.60 ng/m^3. The concentration of PAHs increased by 45% compared to the background concentration during winter Most PAHs, including 1,7-dimethylphenanthrene, fluorene, coronene, which represent 9.05%, 7.94%, and 6.56%, were found in the winter, because of combustion processes. Their influence remains low in comparison to other organic compounds because of high evaporation on warm days (Cincinelli et al., 2007). Other compounds such as 17b(H).21b(H)-hopane (6.4%), 2,6-dimethylphenanthrene (6.5%), or 3,5-dimethylphenanthrene (6.28%) were observed during long-range transport of polluted air masses during ACE or NAO air mass influence. Retene, which is resulting from biogenic emissions, accounts for only 3.18% of total PAHs concentration. As a result, the observation of PAH concentration shows a strong variation with high biogenic activities in the surroundings during summer and high anthropogenic PAHs during pollution episodes from combustion processes in winter.

In total 5 ketones were detected in this study. The ketones concentrations increase significantly from summer to winter by a factor of 2, with an average of 6.9 ng/m^3. The minimum concertation was recorded during the summer of about 0.60 ng/m^3. In contrast, maximum concentration was reached during autumn of about 52 ng/m^3. Ketones species were dominated by 2-heptadecanone, 2-nonadecanone, and 2-pentadecanone, which represent 32.3%, 25%, and 21%, of the total, detected ketones, respectively. The remaining part was made up of 2-hexadecanone and 2-octadecanone, which counts for 15.6%, and 6.2%, respectively. The discrepancy of ketone concentrations in comparison

https://doi.org/10.5194/acp-2021-106
Preprint. Discussion started: 6 April 2021

Atmospheric Chemistry and Physics Discussions

with background chemical composition seems minor from August to October. The trend is completely reversed, as the average concentration was significantly elevated during November and December. During these two months, the concentration increased by 35%. Some spikes detected in November and December are characterized by a change in wind direction, and high wind speeds. These samples, with higher concentrations for 2-heptadecanone and 2-nonadecanone show a strong correlation with temperature. Indeed, this period marks the beginning of winter, with average temperatures dropping as low as 4,5 °C, as shown in Table 1. No correlation between ketones was found with elemental carbon, but the analysis of the data shows a strong correlation only for the night samples with As and K^+. This indicates that a possible source of the ketones is combustion due to residential heating. These data present the first measurement made that shows the influence of combustion in North Africa. Similar conclusions were described by Müller, (1997) who highlighted the anthropogenic influence of ketones during winter.

3.5 Inter-relationship between aerosol components.

A correlation between SO_4^{2-} and NH_4^+ supported the hypothesis of dominant ammonium sulfate particles in the summer, but in winter, as shown in Fig. 9, the trend is more towards ammonium nitrate. Sulfate concentrations during the winter pollution period ranged from 0.11 to 3.87 µg/m^3, as shown in Fig. 6. The high NH_4^+/SO_4^{2-} ratio ranging from 1.5 to 2.1 µg/m^3, is due to the predominance of nitrates over sulfates during winter. Nitrate shows a strong dependency on the temperature at AM5, most likely due to the stability of ammonium nitrate in the atmosphere at low temperatures. During December, nitrates and ammonium remain high, probably due to the influence of temperature that prevents the dissociation of ammonium nitrate particles.

Sulfate attributed to soil origin during dust event was supported by a correlation of nss-SO_4^{2-} with nss-Ca^{2+}, (Fig. 9c) indicating the likely presence of calcite particles most often from the crustal origin. A similar observation was reported by Okada and Kai, (2004), who observed that Desert dust was associated with sulfur compounds and organic matter from surrounding agricultural areas. Indeed, the particles with high sulfate content were accompanied by Ca and were assigned as gypsum particles, which suggesting that the sulfur in these particles originated from a sedimentary source. (Falkovich et al., 2001). On the other hand, the involvement of the Saharan desert was much lower. Ammonium was less enhanced with an average of 0.43 µg/m^3 during dust storms.

On the other hand, Fig. 9 shows two scatter plots indicating the evolution of the chemical species, relationship constituting sea salt over the seasons. Chloride was depleted in the sea salt particles due to the displacement of chloride by sulfate from sulfuric acid, as observed in Fig. 9d since photochemical processes favor sulfate formation during summer. The same scenario has been observed for NO_3^- with a considerable difference during the winter. Indeed, the correlation between sodium and the sum of chloride and nitrate shows the chloride depletion and indicates that the Atlantic Ocean air mass was loaded with aged sea salt. The influence of sea salt remains a significant consequence despite the distance that separates the station from the ocean coast.
A correlation was observed between organic matter and mineral elements such as Ca^{2+}, Mg^{2+}, and Fe (not shown) indicating that mineral dust was also a source of organic matter

3.6 Differences in chemical composition between dust and non-dust events

Mass

https://doi.org/10.5194/acp-2021-106
Preprint. Discussion started: 6 April 2021

Atmospheric Chemistry and Physics Discussions

To investigate the impact of the dust event on the PM_{10} chemical composition, the data has been segregated into two categories dust and non-dust episode. Only selected days with high influence of Saharan air mass were considered to be representative for dust event days. Figure 10 shows the average concentrations during non-dust and dust events. The Long-range transport of mineral dust showed a significant impact on PM_{10} composition. During dust events, PM 10 concentrations were on average 3 times higher, and up to a maximum of 10 times higher, in comparison to non-dust days. Mineral dust was about 5 times higher in comparison to background conditions (Fig. 10a). In addition, RH was lower during dust event days ranging from 20% to 45%, whereas it was 50% to 70% on the non-dust days. Similar results were observed by (Mukherjee et al., 2020) showing the impact of dust on the local meteorological conditions.

Minerals, metals, and ions

Although the North African mineral dust is mainly made up of clay minerals and quartz, the content of calcium carbonates varies depending on the North Africa source (Chiapello et al., 1997; Glaccum and Prospero, 1980). A comparison between Fe/Al and Fe/Ca ratios were used to provide the potential geographical origin of mineral dust according to their chemical composition (Formenti et al., 2014). The variability of the Fe/Al ratio was relatively low (0.92) during non-dust events and decreased to about 0.63 during the dust events, as shown in Fig 10b. The Fe/Ca ratio was also used to make distinctions amongst sources. It was found that the Fe/Ca ratio was 1.4 higher than 1 during dust events, while Fe/Ca was averagely 0.4 during remote background conditions. These ratios, which are robust indicators of large-scale mineral dust source variation, were supported by air mass backward trajectories. The particles during dust events came from the Saharan region of Mauritania and southern Morocco as also indicated by their high Fe/Ca ratio while mineral dust during background conditions as indicated above was of local sources emitted from road-dust or resuspension from agricultural activities.

An increase in the concentration of many ions was also observed during dust events. sulfate, nitrate, calcium, ammonium, showed an increase in the average concentration of about a factor of 4.5 while chloride, magnesium, and potassium experienced an increase in their concentrations by a factor of 5 (Fig 10c, 10d). During dust events, sodium concentration also experienced an increase by a factor of 3. Its correlation with iron and aluminum suggested its possible soil origin. Other metals of anthropogenic origin (not plotted), such as Cu, Ni, and Pb, showed no significant difference between dust and non-dust events.

Organics

Figure (10c) reveals that organic carbon increased averagely during the dust event from 0.5 to 3.5 $\mu g/m^3$. Samples collected during the dust period showed a strong correlation between organic matter and other elements of crustal origin such as nss-Ca^{2+} and nss-Mg^{2+}. The OC/EC ratio was in the range of 4-6 during the dust period, while the ratio was lower than 3 during background conditions which suggest that the organic fraction was affected by desert dust particles. Some organic compounds increase during dust events, especially odd alkanes such as nonaconsane, hentriacontane, heptacosane, and tricosane by a factor of 4. In contrast, elemental carbon remains globally constant with marginal changes (Fig 10e). The PAH fluorene, showed similar concentrations during dust events and background conditions, indicating that Saharan dust was not a significant source. An increase of about 65% was observed for pentacosane, octacosane, hexacosane and decosane. Due to the biodiversity of several plant species and remarkable microbiological activity surrounding the Atlas regions, an increase of some organic

https://doi.org/10.5194/acp-2021-106
Preprint. Discussion started: 6 April 2021


Atmospheric Chemistry and Physics Discussions

compounds and organic matter fraction suggests that mineral dust was loaded with biogenic compounds during dust transport.

3.7 Day and night-time variation

Inorganic ions, mineral dust, and organic matter (OM)

Diurnal variations of various PM_{10} chemical species were analyzed to understand the influence of day and night variations on their concentrations. Figure 11 shows the variation between day and for given chemical species. High concentrations of Al and Fe were observed during the day, compared to the night. This increase seems to be related to an additional source from the resuspension of road dust, due to car traffic during the day. Ca seems stable between day and night. This difference in dust concentration shows the important role that mineral dust plays as a local source. Nevertheless, the transport of mineral dust from the Sahara was controlled by other factors. The study done by Khan et al., 2015 indicates that the penetration of dust into the free troposphere in the Atlas Mountains can also be due to orographic lifting, convection on the mountain slopes, and updrafts in the breeze front. As observed in Fig. 11a), the OC increase during the day was accompanied by a slight increase in alkanes such as pristane, docosane, and nonacosane. These alkanes indicate that the organic fraction was dominated by biogenic sources during the day. The highest concentrations of biotic compounds were reached during the summer.

Elemental carbon (EC), anthropogenic metals, and PAHs

The composition of PM_{10} in the evening is characterized by a high concentration of anthropogenic trace elements. The EC concentrations slightly increased in the evening from 0.22 to 0.26 µg/m^3. Besides, an increase of PAHs and ketones concentrations such as fluorene, retene, and 2-nonadecanone was observed during the night-time. The PAH concentrations during the day and night-time was 0.68 and 0.81 µg/m^3, respectively. In particular, the Fluorene was the most abundant PAH in all the night samples and reached a maximum of 0.82 ng/m^3. A correlation (r^2=0.67) was found between PAHs and EC during night-time indicating their anthropogenic origins. In addition, anthropogenic metals such as Pb, Cr, V, Cr, Ni, and Cu associated with combustion and traffic emissions, increase by a factor of 1.8 during the evening (Fig 11b). Indeed, the anthropogenic influence at the AM5 site occurs during the evening due to two important factors. First, the site is located in a mountainous region influenced by the temperature fluctuation between day and night. The rapid cooling between day and night was accompanied by a change of aerosol sources. This phenomenon is widespread, especially in summer. Second, the variation of the air mass, combined with a change in the height of the boundary layer, contributes to the transport of pollutants from urban sites Fes and Meknes to the AM5 site.

Influence of meteorology

The variation of the meteorological parameters between day and night is a critical factor that can indeed influence the chemical composition of the particles. First, a significant difference in PM_{10} was observed on days when the day and night temperature difference was substantial, for example, on the 12th of August. The concentration decreased during the day (113.01 µg m^{-3}) to 80.4 µg m^{-3} at night. Secondary inorganic aerosols, such as sulfates and nitrate, were characterized by different variations between day and night. On the one hand, the sulfate is highly enhanced during the day, while nitrate shows high concentrations during the night especially. The drop in

https://doi.org/10.5194/acp-2021-106
Preprint. Discussion started: 6 April 2021


Atmospheric Chemistry and Physics Discussions

temperature between the day and the night, especially during the winter, allows for a rapid formation of ammonium nitrate. Sulfate is also sourced from dust resuspension, which explains its increase during the day. However, a correlation between solar radiation and sulfate suggests that photo-oxidation during the day could also be a source of the sulfate increase.

Mechanism of day-night variation

In principle, two mechanisms control the variation between day and night: The wind direction and the boundary layer height. The wind direction plays an important role because it introduces air mass transported from different sources. Indeed, the winds come from all directions, but it is dominated from the west during the day, and by the South-East during the night. High speeds were recorded during the night, up to 17.5 m s^{-1}, mostly associated with marine air masses. This suggests that long-distant transport often occurred during the night while the wind speed during the day was relatively lower. The lower wind speed during the day indicates that the influence of local sources is important. Furthermore, the topography, as well as the embedded valleys, also play a role in the pollution transport during the daytime as shown by Lang et al., (2015). Mountains can give rise to daytime upslope winds and night-time downslope winds. The valley bottom warms during the day, warm air rises the slopes of the surrounding mountains and hills to create a valley breeze. During night-time, radiation from the earth's surface cools the slopes, causing cooler, denser air to drain into the valley. In addition, local boundary layer processes and long-range transport contribute to chemical composition changes (Nair et al., 2007). A similar impact of mountain-valley circulations on air pollution was observed by Bei et al. (2018). Studies at high-altitude sites in southwest India, also found that diurnal variations of aerosol particle concentrations were related to mountain valley winds and the variation in a planetary boundary layer height (Buchunde et al., 2019).

4 Conclusion

In the present study, PM_{10} particulate matter was chemically characterized at the newly established AM5 research station located in the Middle Atlas region (Morocco) at an altitude of 2100 m from August to December 2017. The aerosol chemical composition was evaluated during remote background conditions and the main air mass origins were identified. The data shows an overview of the background chemical composition and the different sources affecting aerosol composition at such a remote high-altitude site. The influence of desert dust was investigated as the site location is close to the Sahara Desert.

Despite the proximity of the site to the Saharan Desert, the influence of the desert on the atmospheric composition at this altitude was only seasonal. PM_{10} mass concentration showed a decreasing trend with high concentrations during summer due to dust events and significantly reduced during autumn due to the washout effect from enhanced rainfall. Four main air mass inflows at the site were identified using back trajectory analysis, with each air mass distinguished by different chemical compositions. The influence of marine air mass from the Atlantic Ocean (NAO) is prevalent at AM5 and made up 53% of all air masses. Background chemical composition in the Middle-Atlas during remote conditions (60 samples) is mainly dominated by locally emitted dust (47%) with high contribution from road dust, Organic Matter (15%), ionic species (16%), organic matter (15%), water content (12%), and indeterminate mass (9%). Biogenic organics contributed up to 7% of the organic matter. Organic matter increased during dust events due to biogenic crustal material emissions. Diurnal variation of PM was related to the variation in a planetary boundary layer, mountain-valley winds as well as changes in different local

https://doi.org/10.5194/acp-2021-106
Preprint. Discussion started: 6 April 2021


Atmospheric Chemistry and Physics Discussions

sources. Mineral dust influenced was seasonal and ranged between 20 and 70% of the mass concentration on PM10 with peaks observed during the summer, accompanied by high concentrations of SO_4^{2-} of up to 1.3 µg/m³.

During winter, PM_{10} concentrations are low, the influence of the desert is weaker, and the marine air masses are more dominant with a mixture of polluted aerosol from the coastal regions of Rabat and Casablanca and sea salt's observed. High concentrations of mineral dust were observed during the daytime due to the resuspension of road dust, while an increase of PAHs and anthropogenic metals such as Pb, Ni, and Cu were found during night-time because of the boundary layer variation. First insight into the aerosol chemical composition during baseline background conditions and over 6 months have been present for the first time in a North Africa high-altitude site. Data show that proximity to desert does not necessarily imply constant exposure to mineral dust. Furthermore, topography and temperature variation at mountain sites control PM concentrations.

This is the first high altitude aerosol characterization study in North Africa which fills an important gap in the African region presently not available. The data from the AM5 sites thus present a reference for aerosol particle composition under regional background conditions as well as during the influence of continental air masses. Several other studies are needed to better understand the influence of the desert on the chemical composition but also the microphysical properties in the Middle Atlas region. In this study, only the chemical composition of bulk PM_{10} particles was investigated, however, the size distribution remains an important factor and should be taken into account in further studies. An additional study on the chemical composition of the urban cities near the AM5, especially in Fes, would allow a better understanding of the anthropogenic influence in the North of Morocco.

https://doi.org/10.5194/acp-2021-106
Preprint. Discussion started: 6 April 2021

Atmospheric Chemistry and Physics Discussions

Data availability. All data will be made available upon request by the authors.

Author contributions. WM, HH, and SE designed the experiment at the AM5 station, KWF and ND collected the samples and performed the data analysis. ND performed the laboratory investigations, compiled the final figures, and prepared the article. All authors reviewed and edited the article and contributed to the discussion.

Competing interests. The authors declare that they have no conflict of interest.

Acknowledgements. The authors would like to thank Ibrahim Ouchen, Sayf El Islam Barcha, and Mehdi El Baramoussi for assistance in sample collection at the AM5. The authors would also acknowledge the support of Kangwei Li, Julia Wilk, Susanne Fuchs, Sylvia Haferkorn, and Cornelia Pielok for their support with the trace metal analysis.

Financial support. This research has been supported by the European Union's Horizon 2020 research and innovation programme (MARSU, grant no. 690958)

The publication of this article was funded by the Open Access Fund of the Leibniz Association.

https://doi.org/10.5194/acp-2021-106
Preprint. Discussion started: 6 April 2021

Atmospheric Chemistry and Physics Discussions

5 References

Ajdour, A., Leghrib, R., Chaoufi, J., Chirmata, A., Menut, L., and Mailler, S.: Towards air quality modeling in Agadir City (Morocco), Materials Today: Proceedings, S2214785319326227, https://doi.org/10.1016/j.matpr.2019.07.438, 2019.

Alastuey, A., Querol, X., Castillo, S., Escudero, M., Avila, A., Cuevas, E., Torres, C., Romero, P., Exposito, F., and Garcia, O.: Characterisation of TSP and PM2.5 at Izaña and Sta. Cruz de Tenerife (Canary Islands, Spain) during a Saharan Dust Episode (July 2002), Atmospheric Environment, 39, 4715–4728, https://doi.org/10.1016/j.atmosenv.2005.04.018, 2005.

Alves, C., Vicente, A., Pio, C., Kiss, G., Hoffer, A., Decesari, S., Prevôt, A. S. H., Minguillón, M. C., Querol, X., Hillamo, R., Spindler, G., and Swietlicki, E.: Organic compounds in aerosols from selected European sites – Biogenic versus anthropogenic sources, Atmospheric Environment, 59, 243–255, https://doi.org/10.1016/j.atmosenv.2012.06.013, 2012.

Ambrose, J. L., Reidmiller, D. R., and Jaffe, D. A.: Causes of high O3 in the lower free troposphere over the Pacific Northwest as observed at the Mt. Bachelor Observatory, Atmospheric Environment, 45, 5302–5315, https://doi.org/10.1016/j.atmosenv.2011.06.056, 2011.

Amodio, M., Catino, S., Dambruoso, P. R., de Gennaro, G., Di Gilio, A., Giungato, P., Laiola, E., Marzocca, A., Mazzone, A., Sardaro, A., and Tutino, M.: Atmospheric Deposition: Sampling Procedures, Analytical Methods, and Main Recent Findings from the Scientific Literature, Advances in Meteorology, 2014, 1–27, https://doi.org/10.1155/2014/161730, 2014.

Arimoto, R., Kim, Y. J., Kim, Y. P., Quinn, P. K., Bates, T. S., Anderson, T. L., Gong, S., Uno, I., Chin, M., Huebert, B. J., Clarke, A. D., Shinozuka, Y., Weber, R. J., Anderson, J. R., Guazzotti, S. A., Sullivan, R. C., Sodeman, D. A., Prather, K. A., and Sokolik, I. N.: Characterization of Asian Dust during ACE-Asia, Global and Planetary Change, 52, 23–56, https://doi.org/10.1016/j.gloplacha.2006.02.013, 2006.

Bei, N., Zhao, L., Wu, J., Li, X., Feng, T., and Li, G.: Impacts of sea-land and mountain-valley circulations on the air pollution in Beijing-Tianjin-Hebei (BTH): A case study, Environmental Pollution, 234, 429–438, https://doi.org/10.1016/j.envpol.2017.11.066, 2018.

Benchrif, A., Guinot, B., Bounakhla, M., Cachier, H., Damnati, B., and Baghdad, B.: Aerosols in Northern Morocco: Input pathways and their chemical fingerprint, Atmospheric Environment, 174, 140–147, https://doi.org/10.1016/j.atmosenv.2017.11.047, 2018.

Bey, I., Jacob, D. J., Yantosca, R. M., Logan, J. A., Field, B. D., Fiore, A. M., Li, Q., Liu, H. Y., Mickley, L. J., and Schultz, M. G.: Global modeling of tropospheric chemistry with assimilated meteorology: Model description and evaluation, J. Geophys. Res., 106, 23073–23095, https://doi.org/10.1029/2001JD000807, 2001.

Birmili, W., Allen, A. G., Bary, F., and Harrison, R. M.: Trace Metal Concentrations and Water Solubility in Size-Fractionated Atmospheric Particles and Influence of Road Traffic, Environ. Sci. Technol., 40, 1144–1153, https://doi.org/10.1021/es0486925, 2006.

Buchunde, P., Safai, P. D., Mukherjee, S., Leena, P. P., Siingh, D., Meena, G. S., and Pandithurai, G.: Characterisation of particulate matter at a high-altitude site in southwest India: Impact of dust episodes, J Earth Syst Sci, 128, 237, https://doi.org/10.1007/s12040-019-1265-8, 2019.

Calvert, J. G.: Glossary of atmospheric chemistry terms (Recommendations 1990), 62, 2167–2219, https://doi.org/10.1351/pac199062112167, 1990.

https://doi.org/10.5194/acp-2021-106
Preprint. Discussion started: 6 April 2021

Campbell, J. F. E., Fletcher, W. J., Joannin, S., Hughes, P. D., Rhanem, M., and Zielhofer, C.: Environmental Drivers of Holocene Forest Development in the Middle Atlas, Morocco, Front. Ecol. Evol., 5, 113, https://doi.org/10.3389/fevo.2017.00113, 2017.

Carter, W., Cockeriii, D., Fitz, D., Malkina, I., Bumiller, K., Sauer, C., Pisano, J., Bufalino, C., and Song, C.: A new environmental chamber for evaluation of gas-phase chemical mechanisms and secondary aerosol formation, Atmospheric Environment, 39, 7768–7788, https://doi.org/10.1016/j.atmosenv.2005.08.040, 2005.

Cavalli, F., Viana, M., Yttri, K. E., and Genberg, J.: Toward a standardised thermal-optical protocol for measuring atmospheric organic and elemental carbon: the EUSAAR protocol, 11, 2010.

Cesari, D., Contini, D., Genga, A., Siciliano, M., Elefante, C., Baglivi, F., and Daniele, L.: Analysis of raw soils and their re-suspended PM10 fractions: Characterisation of source profiles and enrichment factors, Applied Geochemistry, 27, 1238–1246, https://doi.org/10.1016/j.apgeochem.2012.02.029, 2012.

Chatterjee, A., Adak, A., Singh, A. K., Srivastava, M. K., Ghosh, S. K., Tiwari, S., Devara, P. C. S., and Raha, S.: Aerosol Chemistry over a High Altitude Station at Northeastern Himalayas, India, PLoS ONE, 5, e11122, https://doi.org/10.1371/journal.pone.0011122, 2010.

Chiapello, I., Bergametti, G., Chatenet, B., Bousquet, P., Dulac, F., and Soares, E. S.: Origins of African dust transported over the northeastern tropical Atlantic, J. Geophys. Res., 102, 13701–13709, https://doi.org/10.1029/97JD00259, 1997.

Chu, A. K. M., Kwok, R. C. W., and Yu, K. N.: Study of pollution dispersion in urban areas using Computational Fluid Dynamics (CFD) and Geographic Information System (GIS), Environmental Modelling & Software, 20, 273–277, https://doi.org/10.1016/j.envsoft.2004.05.007, 2005.

Cincinelli, A., Bubba, M. D., Martellini, T., Gambaro, A., and Lepri, L.: Gas-particle concentration and distribution of n-alkanes and polycyclic aromatic hydrocarbons in the atmosphere of Prato (Italy), Chemosphere, 68, 472–478, https://doi.org/10.1016/j.chemosphere.2006.12.089, 2007.

Clegg, S. L., Brimblecombe, P., and Wexler, A. S.: Thermodynamic Model of the System H+−NH4+−SO42-−NO3-−H2O at Tropospheric Temperatures, J. Phys. Chem. A, 102, 2137–2154, https://doi.org/10.1021/jp973042r, 1998.

Contini, D., Belosi, F., Gambaro, A., Cesari, D., Stortini, A. M., and Bove, M. C.: Comparison of PM10 concentrations and metal content in three different sites of the Venice Lagoon: An analysis of possible aerosol sources, Journal of Environmental Sciences, 24, 1954–1965, https://doi.org/10.1016/S1001-0742(11)61027-9, 2012.

Council, N. R., Studies, D. on E. and L., Climate, B. on A. S. and, and Pollutants, C. on the S. of I. T. of A.: Global Sources of Local Pollution: An Assessment of Long-Range Transport of Key Air Pollutants to and from the United States, National Academies Press, 249 pp., 2010.

Ding, K., Liu, J., Ding, A., Liu, Q., Zhao, T. L., Shi, J., Han, Y., Wang, H., and Jiang, F.: Uplifting of carbon monoxide from biomass burning and anthropogenic sources to the free troposphere in East Asia, Atmos. Chem. Phys., 15, 2843–2866, https://doi.org/10.5194/acp-15-2843-2015, 2015.

Draxler, R. R.: Evaluation of an Ensemble Dispersion Calculation, 42, 10, 2003.

Du, Y., Xu, X., Chu, M., Guo, Y., and Wang, J.: Air particulate matter and cardiovascular disease: the epidemiological, biomedical and clinical evidence, 8, 12, 2016.

Falkovich, A. H., Ganor, E., Levin, Z., Formenti, P., and Rudich, Y.: Chemical and mineralogical analysis of individual mineral dust particles, J. Geophys. Res., 106, 18029–18036, https://doi.org/10.1029/2000JD900430, 2001.

https://doi.org/10.5194/acp-2021-106
Preprint. Discussion started: 6 April 2021

Fomba, K. W., Müller, K., van Pinxteren, D., Poulain, L., van Pinxteren, M., and Herrmann, H.: Long-term chemical characterization of tropical and marine aerosols at the Cape Verde Atmospheric Observatory (CVAO) from 2007 to 2011, 14, 8883–8904, https://doi.org/10.5194/acp-14-8883-2014, 2014.

Fomba, K. W., Deabji, N., Barcha, S. E. I., Ouchen, I., Elbaramoussi, E. M., El Moursli, R. C., Harnafi, M., El Hajjaji, S., Mellouki, A., and Herrmann, H.: Application of TXRF in monitoring trace metals in particulate matter and cloud water, Atmos. Meas. Tech., 13, 4773–4790, https://doi.org/10.5194/amt-13-4773-2020, 2020.

Formenti, P., Caquineau, S., Desboeufs, K., Klaver, A., Chevaillier, S., Journet, E., and Rajot, J. L.: Mapping the physico-chemical properties of mineral dust in western Africa: mineralogical composition, Atmos. Chem. Phys., 14, 10663–10686, https://doi.org/10.5194/acp-14-10663-2014, 2014.

García, M. I., Rodríguez, S., and Alastuey, A.: Impact of North America on the aerosol composition in the North Atlantic free troposphere, Atmos. Chem. Phys., 17, 7387–7404, https://doi.org/10.5194/acp-17-7387-2017, 2017.

Gherboudj, I., Naseema Beegum, S., and Ghedira, H.: Identifying natural dust source regions over the Middle-East and North-Africa: Estimation of dust emission potential, Earth-Science Reviews, 165, 342–355, https://doi.org/10.1016/j.earscirev.2016.12.010, 2017.

Glaccum, R. A. and Prospero, J. M.: Saharan aerosols over the tropical North Atlantic — Mineralogy, Marine Geology, 37, 295–321, https://doi.org/10.1016/0025-3227(80)90107-3, 1980.

Glasius, M., Hansen, A. M. K., Claeys, M., Henzing, J. S., Jedynska, A. D., Kasper-Giebl, A., Kistler, M., Kristensen, K., Martinsson, J., Maenhaut, W., Nøjgaard, J. K., Spindler, G., Stenström, K. E., Swietlicki, E., Szidat, S., Simpson, D., and Yttri, K. E.: Composition and sources of carbonaceous aerosols in Northern Europe during winter, Atmospheric Environment, 173, 127–141, https://doi.org/10.1016/j.atmosenv.2017.11.005, 2018.

Golly, B., Waked, A., Weber, S., Samake, A., Jacob, V., Conil, S., Rangognio, J., Chrétien, E., Vagnot, M.-P., Robic, P.-Y., Besombes, J.-L., and Jaffrezo, J.-L.: Organic markers and OC source apportionment for seasonal variations of PM2.5 at 5 rural sites in France, Atmospheric Environment, 198, 142–157, https://doi.org/10.1016/j.atmosenv.2018.10.027, 2019.

Iinuma, Y., Brüggemann, E., Gnauk, T., Müller, K., Andreae, M. O., Helas, G., Parmar, R., and Herrmann, H.: Source characterization of biomass burning particles: The combustion of selected European conifers, African hardwood, savanna grass, and German and Indonesian peat, J. Geophys. Res., 112, D08209, https://doi.org/10.1029/2006JD007120, 2007.

Iinuma, Y., Engling, G., Puxbaum, H., and Herrmann, H.: A highly resolved anion-exchange chromatographic method for determination of saccharidic tracers for biomass combustion and primary bio-particles in atmospheric aerosol, Atmospheric Environment, 43, 1367–1371, https://doi.org/10.1016/j.atmosenv.2008.11.020, 2009.

Inchaouh, M.: STATE OF AMBIENT AIR QUALITY IN MARRAKECH CITY (MOROCCO) OVER THE PERIOD 2009 – 2012, geomate, https://doi.org/10.21660/2017.29.1254, 2017.

Jaenicke, R.: Über die Dynamik atmosphärischer Aitkenteilchen, Berichte der Bunsengesellschaft für physikalische Chemie, 82, 1198–1202, https://doi.org/10.1002/bbpc.19780821126, 1978.

Jaenicke, R.: Abundance of Cellular Material and Proteins in the Atmosphere, 308, 73–73, https://doi.org/10.1126/science.1106335, 2005.

Jia, G., Shevliakova, E., Artaxo, P., Noblet-Ducoudré, N. D., Houghton, R., Anderegg, W., Bastos, A., Bernsten, T. K., Cai, P., Calvin, K., Klein, C. D., Humpenöder, F., Kanter, D.,

https://doi.org/10.5194/acp-2021-106
Preprint. Discussion started: 6 April 2021

McDermid, S., Peñuelas, J., Pradhan, P., Quesada, B., Roe, S., Bernier, P., Espinoza, J. C., Semenov, S., and Xu, X.: SPM2 Land–climate interactions, 118, n.d.

Kchih, H., Perrino, C., and Cherif, S.: Investigation of Desert Dust Contribution to Source Apportionment of PM10 and PM2.5 from a Southern Mediterranean Coast, Aerosol Air Qual. Res., 15, 454–464, https://doi.org/10.4209/aaqr.2014.10.0255, 2015.

Khrissi, S., Bejjit, L., Haddad, M., Falguères, C., Ait Lyazidi, S., and El Amraoui, M.: Study of marbles from Middle Atlas (Morocco): elemental, mineralogical and structural analysis, IOP Conf. Ser.: Mater. Sci. Eng., 353, 012013, https://doi.org/10.1088/1757-899X/353/1/012013, 2018.

King, M. D., Menzel, W. P., Kaufman, Y. J., Tanre, D., Bo-Cai Gao, Platnick, S., Ackerman, S. A., Remer, L. A., Pincus, R., and Hubanks, P. A.: Cloud and aerosol properties, precipitable water, and profiles of temperature and water vapor from MODIS, IEEE Trans. Geosci. Remote Sensing, 41, 442–458, https://doi.org/10.1109/TGRS.2002.808226, 2003.

Knippertz, P., Deutscher, C., Kandler, K., Müller, T., Schulz, O., and Schütz, L.: Dust mobilization due to density currents in the Atlas region: Observations from the Saharan Mineral Dust Experiment 2006 field campaign, J. Geophys. Res., 112, D21109, https://doi.org/10.1029/2007JD008774, 2007.

Kreidenweis, S. M., Petters, M. D., and DeMott, P. J.: Single-parameter estimates of aerosol water content, Environ. Res. Lett., 3, 035002, https://doi.org/10.1088/1748-9326/3/3/035002, 2008.

Lang, M. N., Gohm, A., and Wagner, J. S.: The impact of embedded valleys on daytime pollution transport over a mountain range, 17, 2015.

Leena, P. P., Vijayakumar, K., Anilkumar, V., and Pandithurai, G.: Analysing temporal variability of particulate matter and possible contributing factors over Mahabaleshwar, a high-altitude station in Western Ghats, India, Journal of Atmospheric and Solar-Terrestrial Physics, 164, 105–115, https://doi.org/10.1016/j.jastp.2017.08.013, 2017.

Leng, C., Zhang, Q., Tao, J., Zhang, H., Zhang, D., Xu, C., Li, X., Kong, L., Cheng, T., Zhang, R., Yang, X., Chen, J., Qiao, L., Lou, S., Wang, H., and Chen, C.: Impacts of new particle formation on aerosol cloud condensation nuclei (CCN) activity in Shanghai: case study, Atmos. Chem. Phys., 14, 11353–11365, https://doi.org/10.5194/acp-14-11353-2014, 2014.

Liang, Q., Jaeglé, L., Jaffe, D. A., Weiss-Penzias, P., Heckman, A., and Snow, J. A.: Long-range transport of Asian pollution to the northeast Pacific: Seasonal variations and transport pathways of carbon monoxide: TRANSPORT PATHWAYS TO THE NORTHEAST PACIFIC, J. Geophys. Res., 109, https://doi.org/10.1029/2003JD004402, 2004.

Lugauer, M., Baltensperger, U., Furger, M., Gaggeler, H. W., Jost, D. T., Schwikowski, M., and Wanner, H.: Aerosol transport to the high Alpine sites Jungfraujoch (3454 m asl) and Colle Gnifetti (4452 m asl), Tellus B, 50, 76–92, https://doi.org/10.1034/j.1600-0889.1998.00006.x, 1998.

Maenhaut, W., Raes, N., Chi, X., Cafmeyer, J., Wang, W., and Salma, I.: Chemical composition and mass closure for fine and coarse aerosols at a kerbside in Budapest, Hungary, in spring 2002, 34, 290–296, https://doi.org/10.1002/xrs.820, 2005.

Marenco, F., Bonasoni, P., Calzolari, F., Ceriani, M., Chiari, M., Cristofanelli, P., D'Alessandro, A., Fermo, P., Lucarelli, F., Mazzei, F., Nava, S., Piazzalunga, A., Prati, P., Valli, G., and Vecchi, R.: Characterization of atmospheric aerosols at Monte Cimone, Italy, during summer 2004: Source apportionment and transport mechanisms, J. Geophys. Res., 111, D24202, https://doi.org/10.1029/2006JD007145, 2006.

Marzi, R., Torkelson, B. E., and Olson, R. K.: A revised carbon preference index, Organic Geochemistry, 20, 1303–1306, https://doi.org/10.1016/0146-6380(93)90016-5, 1993.

https://doi.org/10.5194/acp-2021-106
Preprint. Discussion started: 6 April 2021

Miche, H., Saracco, G., Mayer, A., Qarqori, K., Rouai, M., Dekayir, A., Chalikakis, K., and Emblanch, C.: Hydrochemical constraints between the karst Tabular Middle Atlas Causses and the Saïs basin (Morocco): implications of groundwater circulation, Hydrogeol J, 26, 71–87, https://doi.org/10.1007/s10040-017-1675-0, 2018.

Minguillón, M. C., Querol, X., Alastuey, A., Monfort, E., and Miró, J. V.: PM sources in a highly industrialised area in the process of implementing PM abatement technology. Quantification and evolution, 9, 1071–1081, https://doi.org/10.1039/B705474B, 2007.

Mounir, S., Saoud, N., Charroud, M., Mounir, K., and Choukrad, J.: The Middle Atlas Geological karsts forms: Towards Geosites characterization, Oil Gas Sci. Technol. – Rev. IFP Energies nouvelles, 74, 17, https://doi.org/10.2516/ogst/2018089, 2019.

Mukherjee, S., Singla, V., Meena, G. S., Aslam, M. Y., Safai, P. D., Buchunde, P., Vasudevan, A. K., Jena, C. K., Ghude, S. D., Dani, K., and Pandithurai, G.: Sub micron aerosol variability and its ageing process at a high altitude site in India: Impact of meteorological conditions, Environmental Pollution, 265, 115019, https://doi.org/10.1016/j.envpol.2020.115019, 2020.

Müller, K.: Determination of aldehydes and ketones in the atmosphere — A comparative long time study at an urban and a rural site in Eastern Germany, Chemosphere, 35, 2093–2106, https://doi.org/10.1016/S0045-6535(97)00267-1, 1997.

Nair, V. S., Moorthy, K. K., Alappattu, D. P., Kunhikrishnan, P. K., George, S., Nair, P. R., Babu, S. S., Abish, B., Satheesh, S. K., Tripathi, S. N., Niranjan, K., Madhavan, B. L., Srikant, V., Dutt, C. B. S., Badarinath, K. V. S., and Reddy, R. R.: Wintertime aerosol characteristics over the Indo-Gangetic Plain (IGP): Impacts of local boundary layer processes and long-range transport: WINTER AEROSOLS OVER INDO-GANGETIC PLAIN, J. Geophys. Res., 112, n/a-n/a, https://doi.org/10.1029/2006JD008099, 2007.

Nerriere, É., Guegan, H., Bordigoni, B., Hautemaniere, A., Momas, I., Ladner, J., Target, A., Lameloise, P., Delmas, V., Personnaz, M.-B., Koutrakis, P., and Zmirou-Navier, D.: Spatial heterogeneity of personal exposure to airborne metals in French urban areas, Science of The Total Environment, 373, 49–56, https://doi.org/10.1016/j.scitotenv.2006.10.042, 2007.

Neusüss, C., Pelzing, M., Plewka, A., and Herrmann, H.: A new analytical approach for size-resolved speciation of organic compounds in atmospheric aerosol particles: Methods and first results, J. Geophys. Res., 105, 4513–4527, https://doi.org/10.1029/1999JD901038, 2000.

Noulas, C., Tziouvalekas, M., and Karyotis, T.: Zinc in soils, water and food crops, Journal of Trace Elements in Medicine and Biology, 49, 252–260, https://doi.org/10.1016/j.jtemb.2018.02.009, 2018.

Nourelbait, M., Rhoujjati, A., Benkaddour, A., Carré, M., Eynaud, F., Martinez, P., and Cheddadi, R.: Climate change and ecosystems dynamics over the last 6000 years in the Middle Atlas, Morocco, Clim. Past, 12, 1029–1042, https://doi.org/10.5194/cp-12-1029-2016, 2016.

Okada, K. and Kai, K.: Atmospheric mineral particles collected at Qira in the Taklamakan Desert, China, Atmospheric Environment, 38, 6927–6935, https://doi.org/10.1016/j.atmosenv.2004.03.078, 2004.

Okamoto, S. and Tanimoto, H.: A review of atmospheric chemistry observations at mountain sites, Prog. in Earth and Planet. Sci., 3, 34, https://doi.org/10.1186/s40645-016-0109-2, 2016.

Pacyna, E. G., Pacyna, J. M., Fudala, J., Strzelecka-Jastrzab, E., Hlawiczka, S., Panasiuk, D., Nitter, S., Pregger, T., Pfeiffer, H., and Friedrich, R.: Current and future emissions of selected heavy metals to the atmosphere from anthropogenic sources in Europe,

Atmospheric Environment, 41, 8557–8566, https://doi.org/10.1016/j.atmosenv.2007.07.040, 2007.

Parrish, D. D., Law, K. S., Staehelin, J., Derwent, R., Cooper, O. R., Tanimoto, H., Volz-Thomas, A., Gilge, S., Scheel, H.-E., Steinbacher, M., and Chan, E.: Long-term changes in lower tropospheric baseline ozone concentrations at northern mid-latitudes, Atmos. Chem. Phys., 12, 11485–11504, https://doi.org/10.5194/acp-12-11485-2012, 2012.

Perrino, C., Catrambone, M., Dalla Torre, S., Rantica, E., Sargolini, T., and Canepari, S.: Seasonal variations in the chemical composition of particulate matter: a case study in the Po Valley. Part I: macro-components and mass closure, Environ Sci Pollut Res, 21, 3999–4009, https://doi.org/10.1007/s11356-013-2067-1, 2014.

Pietrogrande, M. C., Mercuriali, M., Perrone, M. G., Ferrero, L., Sangiorgi, G., and Bolzacchini, E.: Distribution of n -Alkanes in the Northern Italy Aerosols: Data Handling of GC-MS Signals for Homologous Series Characterization, Environ. Sci. Technol., 44, 4232–4240, https://doi.org/10.1021/es1001242, 2010.

Pietrogrande, M. C., Abbaszade, G., Schnelle-Kreis, J., Bacco, D., Mercuriali, M., and Zimmermann, R.: Seasonal variation and source estimation of organic compounds in urban aerosol of Augsburg, Germany, Environmental Pollution, 159, 1861–1868, https://doi.org/10.1016/j.envpol.2011.03.023, 2011.

van Pinxteren, D., Brüggemann, E., Gnauk, T., Müller, K., Thiel, C., and Herrmann, H.: A GIS based approach to back trajectory analysis for the source apportionment of aerosol constituents and its first application, J Atmos Chem, 67, 1–28, https://doi.org/10.1007/s10874-011-9199-9, 2010.

van Pinxteren, M., Fiedler, B., van Pinxteren, D., Iinuma, Y., Körtzinger, A., and Herrmann, H.: Chemical characterization of sub-micrometer aerosol particles in the tropical Atlantic Ocean: marine and biomass burning influences, J Atmos Chem, 72, 105–125, https://doi.org/10.1007/s10874-015-9307-3, 2015.

Pope, C. A., Cohen, A. J., and Burnett, R. T.: Cardiovascular Disease and Fine Particulate Matter: Lessons and Limitations of an Integrated Exposure–Response Approach, Circ Res, 122, 1645–1647, https://doi.org/10.1161/CIRCRESAHA.118.312956, 2018.

Putero, D., Cristofanelli, P., Marinoni, A., Adhikary, B., Duchi, R., Shrestha, S. D., Verza, G. P., Landi, T. C., Calzolari, F., Busetto, M., Agrillo, G., Biancofiore, F., Di Carlo, P., Panday, A. K., Rupakheti, M., and Bonasoni, P.: Seasonal variation of ozone and black carbon observed at Paknajol, an urban site in the Kathmandu Valley, Nepal, Atmos. Chem. Phys., 15, 13957–13971, https://doi.org/10.5194/acp-15-13957-2015, 2015.

Rodrıguez, S., Gonzalez, Y., Cuevas, E., Ramos, R., Romero, P. M., Abreu-Afonso, J., and Redondas, A.: Atmospheric nanoparticle observations in the low free troposphere during upward orographic flows at Izan˜ a Mountain Observatory, 17, 2009.

Royaume du Maroc: Plan national de lutte contre le réchauffement climatique, Ministère de l'Énergie, des Mines, de l'Eau et de l'Environnement, Rabat, 2009.

Satheesh, S. K. and Krishna Moorthy, K.: Radiative effects of natural aerosols: A review, Atmospheric Environment, 39, 2089–2110, https://doi.org/10.1016/j.atmosenv.2004.12.029, 2005.

Satsangi, P. G., Chavan, S. P., Rao, P. S. P., and Safai, P. D.: Chemical characterization of particulate matter at Sinhagad, a high altitude station in Pune, India, 9, 2014.

Scerri, M. M., Kandler, K., and Weinbruch, S.: Disentangling the contribution of Saharan dust and marine aerosol to PM10 levels in the Central Mediterranean, Atmospheric Environment, 147, 395–408, https://doi.org/10.1016/j.atmosenv.2016.10.028, 2016.

Song, Q., Christiani, D., XiaorongWang, and Ren, J.: The Global Contribution of Outdoor Air Pollution to the Incidence, Prevalence, Mortality and Hospital Admission for Chronic

https://doi.org/10.5194/acp-2021-106
Preprint. Discussion started: 6 April 2021

Atmospheric Chemistry and Physics Discussions

Obstructive Pulmonary Disease: A Systematic Review and Meta-Analysis, IJERPH, 11, 11822–11832, https://doi.org/10.3390/ijerph111111822, 2014.

Stein, A. F., Draxler, R. R., Rolph, G. D., Stunder, B. J. B., Cohen, M. D., and Ngan, F.: NOAA's HYSPLIT Atmospheric Transport and Dispersion Modeling System, Bull. Amer. Meteor. Soc., 96, 2059–2077, https://doi.org/10.1175/BAMS-D-14-00110.1, 2015.

Tahiri, A., Diouri, M., Steli, H., Marsli, I., Meziane, R., and Ben-tayeb, A.: Desert aerosol optical properties in Morocco, es, 4, 63–78, https://doi.org/10.12988/es.2016.631, 2016.

Tahri, M., Bounakhla, M., Zghaïd, M., Benchrif, A., Zahry, F., Noack, Y., and Benyaïch, F.: TXRF characterization and source identification by positive matrix factorization of airborne particulate matter sampled in Kenitra City (Morocco): TXRF characterization and source identification in Kenitra City, Morocco, 42, 284–289, https://doi.org/10.1002/xrs.2484, 2013.

Tiwari, S., Hopke, P. K., Pipal, A. S., Srivastava, A. K., Bisht, D. S., Tiwari, S., Singh, A. K., Soni, V. K., and Attri, S. D.: Intra-urban variability of particulate matter (PM2.5 and PM10) and its relationship with optical properties of aerosols over Delhi, India, Atmospheric Research, 166, 223–232, https://doi.org/10.1016/j.atmosres.2015.07.007, 2015.

Turpin, B. J. and Lim, H.-J.: Species Contributions to PM2.5 Mass Concentrations: Revisiting Common Assumptions for Estimating Organic Mass, Aerosol Science and Technology, 35, 602–610, https://doi.org/10.1080/02786820119445, 2001.

Viana, M., Pandolfi, M., Minguillón, M. C., Querol, X., Alastuey, A., Monfort, E., and Celades, I.: Inter-comparison of receptor models for PM source apportionment: Case study in an industrial area, Atmospheric Environment, 42, 3820–3832, https://doi.org/10.1016/j.atmosenv.2007.12.056, 2008.

Wang, Y. Q., Zhang, X. Y., Sun, J. Y., Zhang, X. C., Che, H. Z., and Li, Y.: Spatial and temporal variations of the concentrations of PM 10 , PM 2.5 and PM 1 in China, Atmos. Chem. Phys., 15, 13585–13598, https://doi.org/10.5194/acp-15-13585-2015, 2015.

Waples, D. W.: Correlations, in: Geochemistry in Petroleum Exploration, edited by: Waples, D. W., Springer Netherlands, Dordrecht, 155–180, https://doi.org/10.1007/978-94-009-5436-6_10, 1985.

Wedepohl, K. H.: The composition of the continental crust, 16, 1995.

Weiss-Penzias, P., Jaffe, D. A., Swartzendruber, P., Dennison, J. B., Chand, D., Hafner, W., and Prestbo, E.: Observations of Asian air pollution in the free troposphere at Mount Bachelor Observatory during the spring of 2004: OBSERVATIONS AT MT. BACHELOR OBSERVATORY, J. Geophys. Res., 111, n/a-n/a, https://doi.org/10.1029/2005JD006522, 2006.

Yttri, K. E., Simpson, D., Bergström, R., Kiss, G., Szidat, S., Ceburnis, D., Eckhardt, S., Hueglin, C., Nøjgaard, J. K., Perrino, C., Pisso, I., Prevot, A. S. H., Putaud, J.-P., Spindler, G., Vana, M., Zhang, Y.-L., and Aas, W.: The EMEP Intensive Measurement Period campaign, 2008–2009: characterizing carbonaceous aerosol at nine rural sites in Europe, Atmos. Chem. Phys., 19, 4211–4233, https://doi.org/10.5194/acp-19-4211-2019, 2019.

Zhang, J. M., Wang, T., Ding, A. J., Zhou, X. H., Xue, L. K., Poon, C. N., Wu, W. S., Gao, J., Zuo, H. C., Chen, J. M., Zhang, X. C., and Fan, S. J.: Continuous measurement of peroxyacetyl nitrate (PAN) in suburban and remote areas of western China, Atmospheric Environment, 43, 228–237, https://doi.org/10.1016/j.atmosenv.2008.09.070, 2009.

Zhao, Z., Cao, J., Shen, Z., Xu, B., Zhu, C., Chen, L.-W. A., Su, X., Liu, S., Han, Y., Wang, G., and Ho, K.: Aerosol particles at a high-altitude site on the Southeast Tibetan Plateau, China: Implications for pollution transport from South Asia: AEROSOL PARTICLES IN SOUTHEAST TP, J. Geophys. Res. Atmos., 118, 11,360-11,375, https://doi.org/10.1002/jgrd.50599, 2013.

https://doi.org/10.5194/acp-2021-106
Preprint. Discussion started: 6 April 2021

Atmospheric Chemistry and Physics Discussions

1200 **Figure 1.** (A) Location map of AM5 site in the Middle-Atlas; (B) Photo of the AM5 site

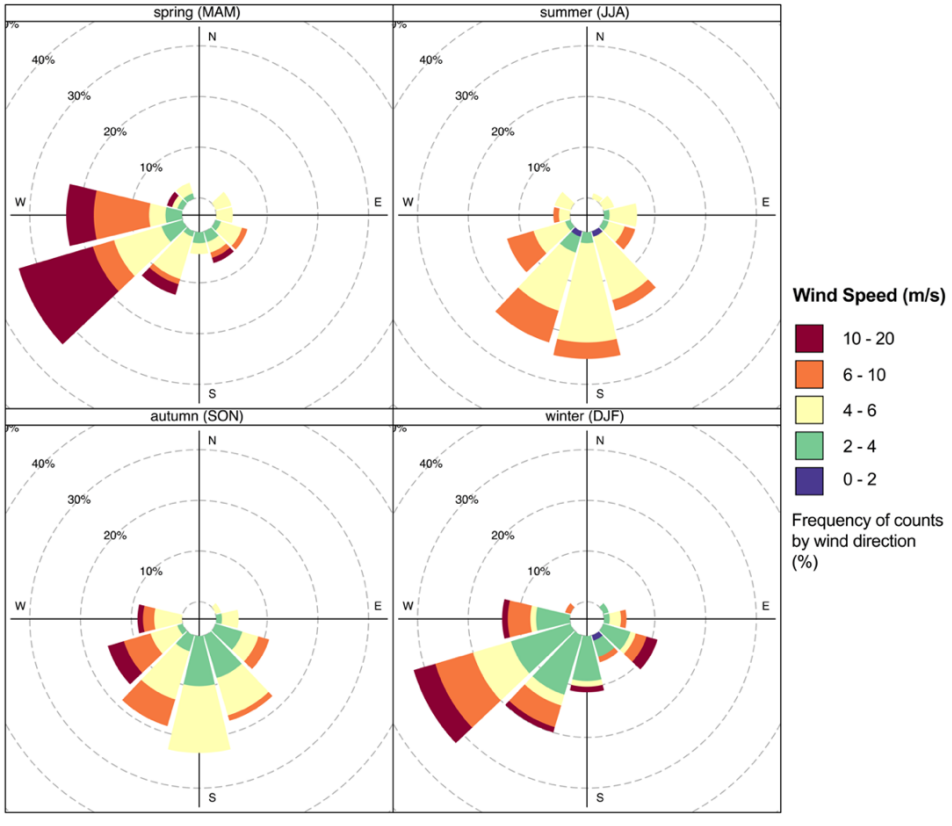

Figure 2. Seasonal wind rose plots at AM5

https://doi.org/10.5194/acp-2021-106
Preprint. Discussion started: 6 April 2021

Atmospheric Chemistry and Physics Discussions

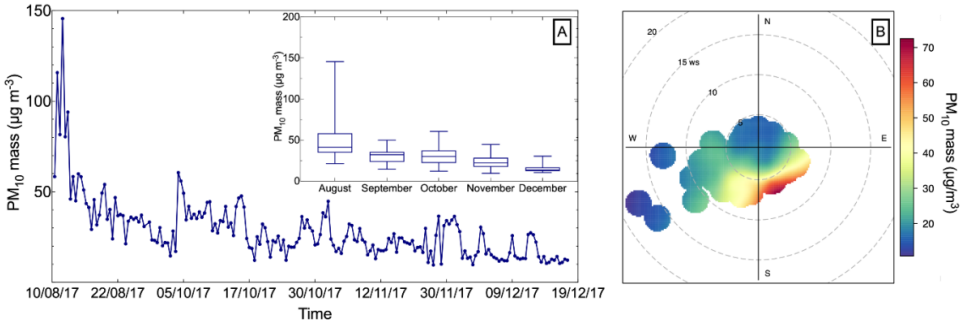

1205

Figure 3. (A) Time series of daily PM_{10} mass and Box plot of monthly averages of PM_{10} mass; (B) Pollution rose of PM_{10} mass

1210

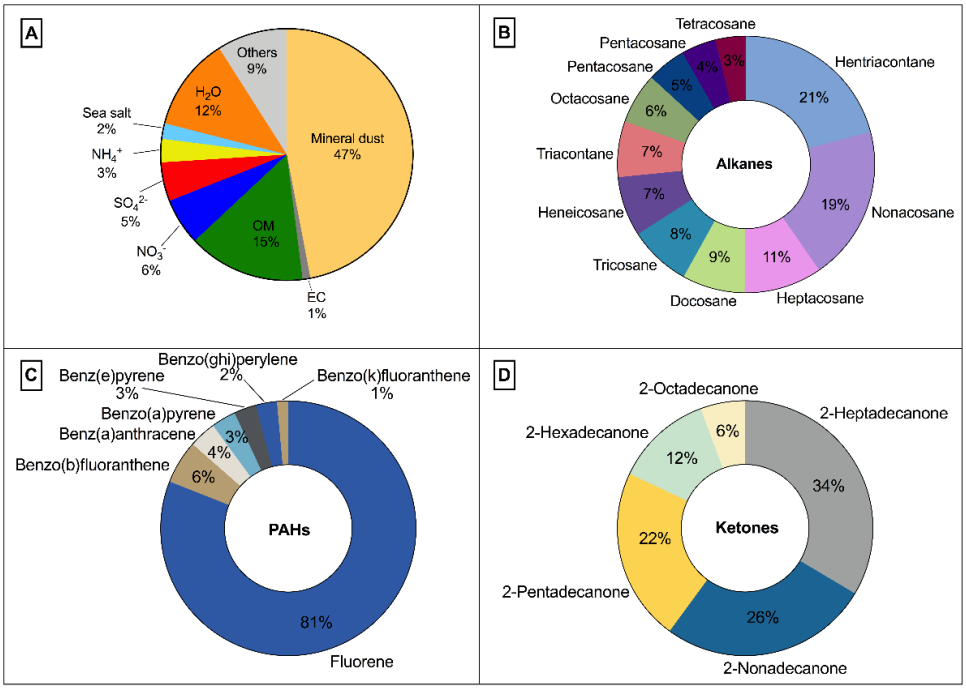

Figure 4. (A) Typical background chemical composition average at AM5 station (60 samples); (B) Aliphatic hydrocarbons; (C) Polycyclic aromatic hydrocarbons; (D) Ketones; identified compounds

https://doi.org/10.5194/acp-2021-106
Preprint. Discussion started: 6 April 2021

Atmospheric Chemistry and Physics Discussions

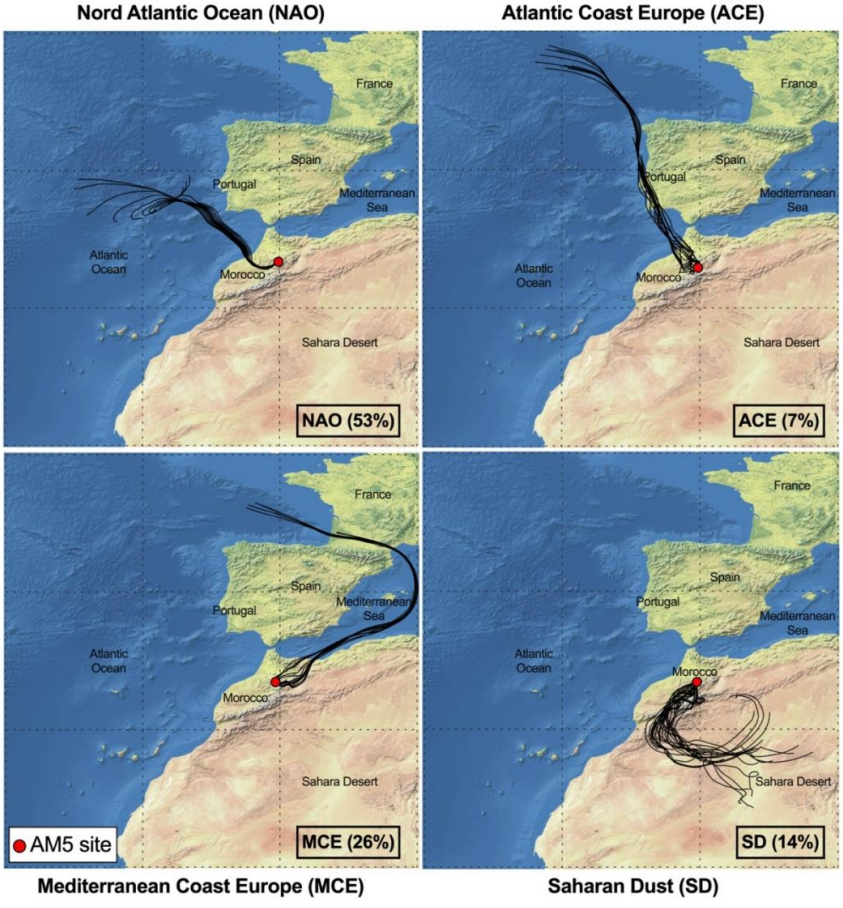

1215 **Figure 5.** Typical 96h air mass back trajectory ensembles performed for AM5 during routine samples periods (aerosol type and PM_{10} mass concentration are given in parentheses)

https://doi.org/10.5194/acp-2021-106
Preprint. Discussion started: 6 April 2021

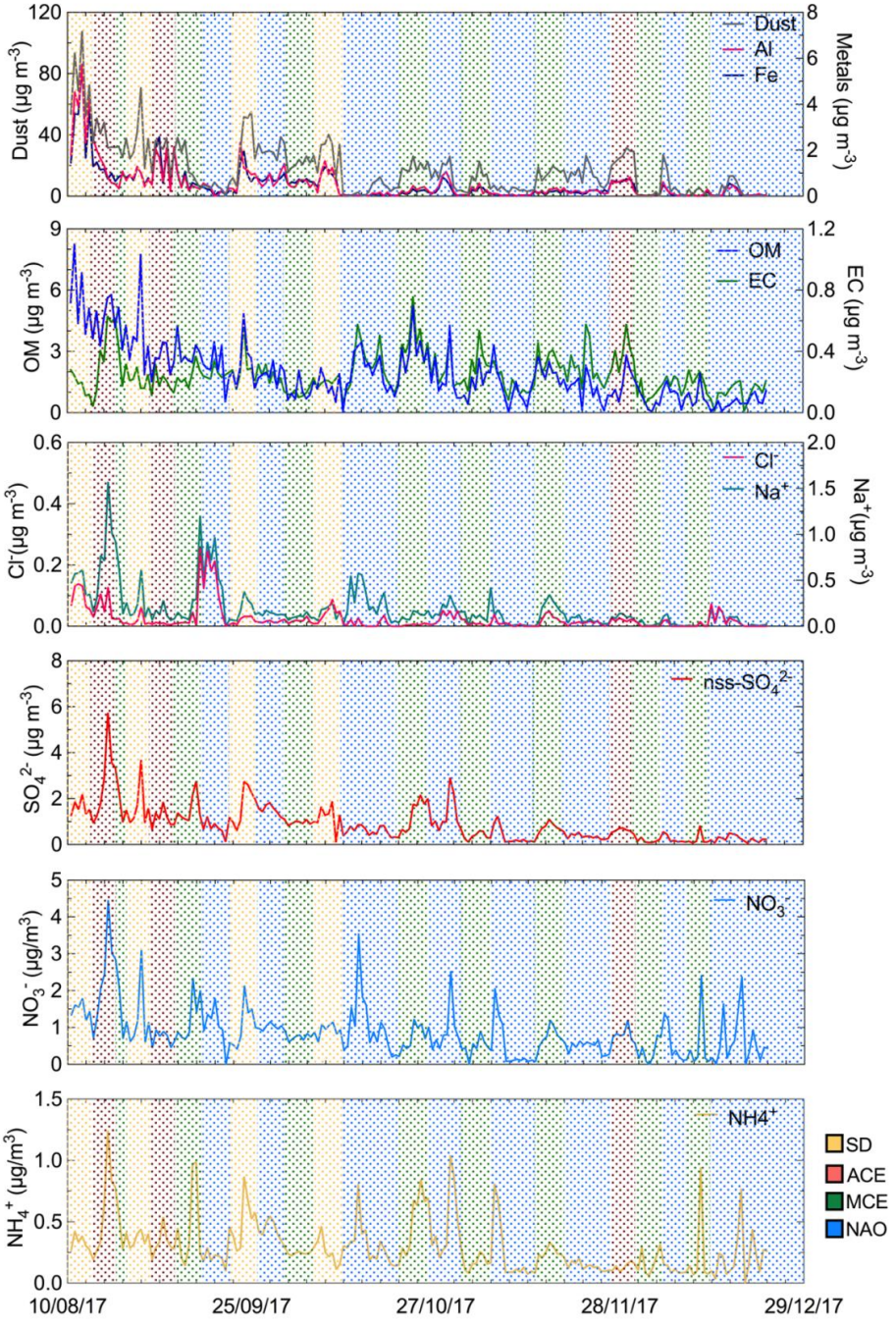

1220 **Figure 6.** Time series of major aerosol chemical constituents in PM_{10} filter samples collected from August to December 2017

https://doi.org/10.5194/acp-2021-106
Preprint. Discussion started: 6 April 2021

Atmospheric Chemistry and Physics Discussions

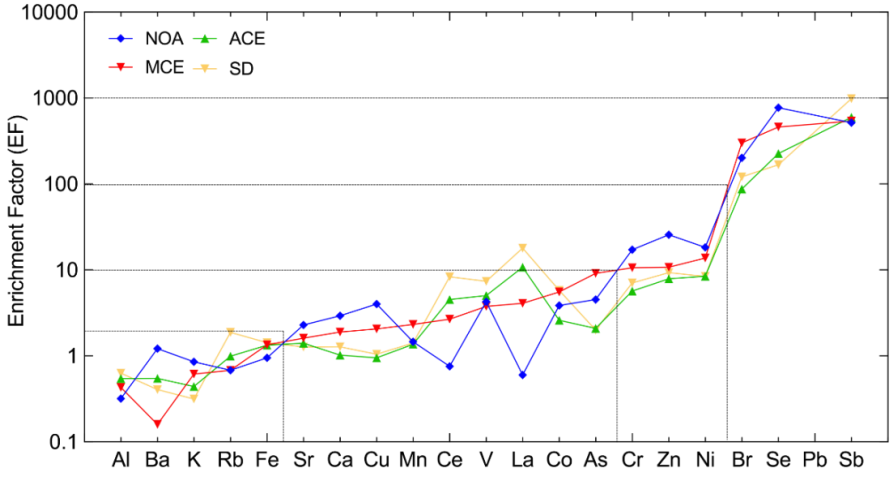

Figure 7. Enrichment factor analysis according to air mass

1225

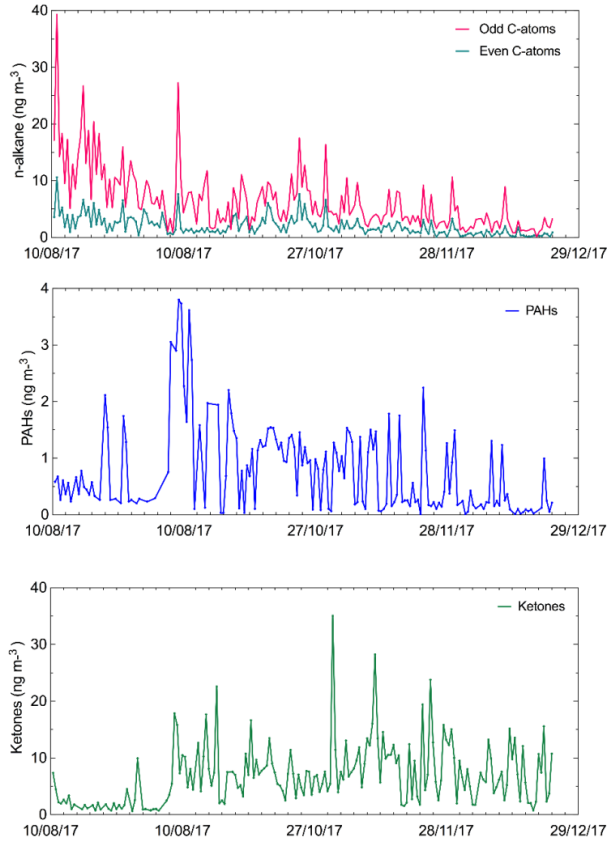

Figure 8. Time series of organic compounds at AM5 during the sampling period

https://doi.org/10.5194/acp-2021-106
Preprint. Discussion started: 6 April 2021

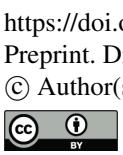

Atmospheric Chemistry and Physics Discussions

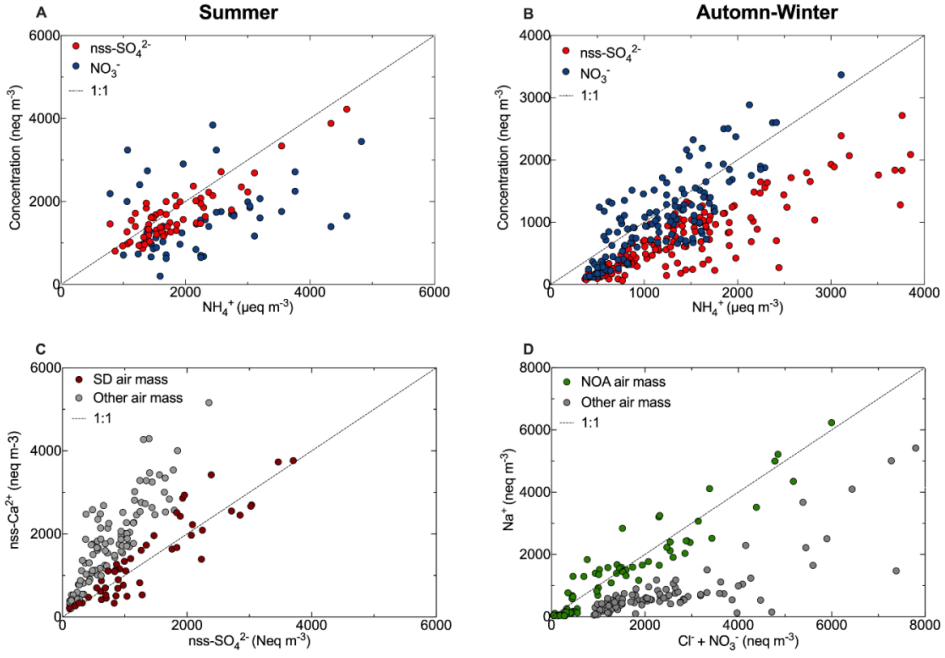

1230 **Figure 9.** Correlations between various compound and elements according to seasons

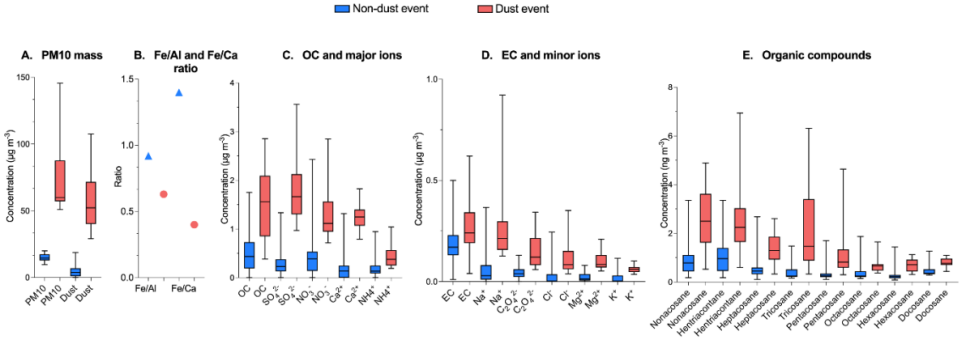

1235 **Figure 10.** Boxplot in the period of dust and non-dust events for concentrations of **(A)** PM_{10} mass and mineral dust; **(B)** Fe/Al and Fe/Ca ratio **(C)** OC and major water-soluble ions, **(D)** EC and minor water-soluble ions; and **(E)** organic compounds

https://doi.org/10.5194/acp-2021-106
Preprint. Discussion started: 6 April 2021

Atmospheric Chemistry and Physics Discussions

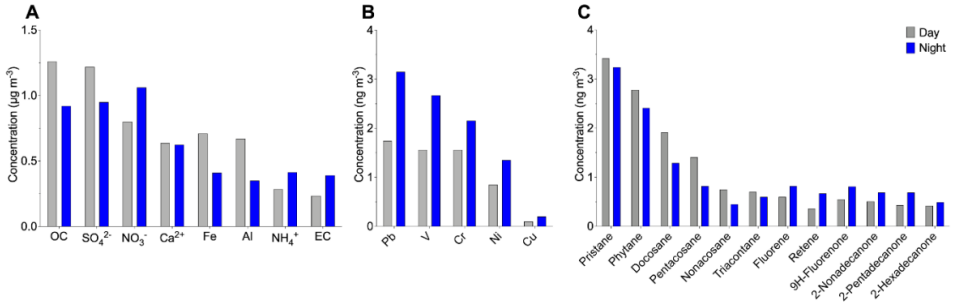

1240 **Figure 11.** Day and night-time variation of (A) OC, EC, ionic chemical species, (B) anthropogenic metals, and (C) Organic compounds such as alkanes, PAHs and ketones.

https://doi.org/10.5194/acp-2021-106
Preprint. Discussion started: 6 April 2021

Atmospheric Chemistry and Physics Discussions

Table 1. Meteorological parameters over Middle-Atlas from summer 2017 to spring 2018

Meteorological Parameter	Period			
	Summer 2017	Autumn 2017	Winter 2018	Spring 2018
Temperature (°C)				
Mean	24	17	5	10
Min	19	10	-1	3
Max	26	21	7	13
Wind speed (km/h)				
Mean	18	18	20	26
Min	6	8	7	12
Max	29	59	59	71
Relative humidity (%)				
Mean	37	39	74	62
Max	80	92	97	94
Rainfall (mm)	37	63	141	56
Wind direction (degrees)	182	185	205	221
Visibility (km)	10	10	9	9
Pressure (mbar)	1 022	1 025	1 034	1 027

Table 2. Comparison of different methods for dust estimation

Method	Mean	Max	Min	Std	Equation	Reference
Method 1	24.5	132.1	5.19	18.2	$MD_1 = PM10\ mass - (\sum All\ detected\ element)$	Fomba et al. (2014)
Method 2	19.9	112.3	0.46	17.8	$MD_2 = 1.16\,(1.90\,Al + 2.15\,Si + 1.41\,Ca + 2.09\,Fe + 1.67\,Ti)$	Maenhaut et al., 2005)
Method 3	18.9	104.9	0.20	18.9	$MD_3 = 4\left(\frac{Al}{27}\right)51 + 100\left(\frac{Ca}{40}\right) + 84\left(\frac{Mg}{24}\right) + 80\left(\frac{Ti}{48}\right) + 87\left(\frac{Mn}{55}\right) + 80\left(\frac{Fe}{56}\right)$	Minguillón et al. (2007); Nerriere et al. (2007)
Method 4	15.5	91.4	0.13	13.9	$MD_4 = 2.1\,Al + 2.9\,Si + 1.4\ nss - Ca^{2+} + 1.4\ nss - Mg^{2+} + 1.43\,Fe + 1.55\,K + 1.58\,Mn$	Cesari et al. (2012); Marenco et al. (2006); Perrino et al. (2014)

https://doi.org/10.5194/acp-2021-106
Preprint. Discussion started: 6 April 2021

Atmospheric Chemistry and Physics Discussions

1260

1265

Table 3. Average mass concentration of PM_{10} from other sites reported in the literature according to altitude.

No.	Site	Site type	Sampling Period	Altitude (m)	PM_{10} ($\mu g/m^3$)	References
1	Lhasa, Tibet	High altitude	Jan-Feb 2006	3663	37.7	Wang et al., 2015
2	Izaña, Canary Islands	High altitude	Feb 2008-Aug 2013	2400	46.2	García et al., 2017
3	Darjeeling, India	High altitude	Jan-Dec 2005	2200	29.5	Chatterjee et al., 2010
4	**Atlas (AM5), Morocco**	High altitude	Aug-Dec 2017	2100	29.1	Present study
5	Sinhagad, India	High altitude	Nov 2008-Apr 2009	1455	35.8	Satsangi et al., 2014
6	Kathmandu, Nepal	High altitude	Feb 2013-Jan 2014	1400	169	Putero et al., 2015
7	Mahabaleshwar, India	High altitude	Jun 2012-May 2013	1348	37.7	Leena et al., 2017
8	Dehli, India	Urban	Dec 2011-Jun 2013	216	232.1	Tiwari et al., 2015
9	Tetouan, Morocco	Urban	May 2011-April 2012	105	31.6	Benchrif et al., 2018
10	Gozo, Malta	Marine	Mar 2012-May 2013	114	18.2	Scerri et al., 2016
11	Tunis, Tunisia	Urban	Jun-Jul 2008	40	58.7	Kchih et al., 2015
12	CVAO, Cap Verde	Marine	Jan 2007-Dec 2011	10	47.2	Fomba et al., 2014

https://doi.org/10.5194/acp-2021-106
Preprint. Discussion started: 6 April 2021

Atmospheric Chemistry and Physics Discussions

1270

Table 4. Mean, max, min, and standard deviation (Std) of chemical species during background conditions

Elements ($ng\ m^{-3}$)	Mean	Std	Min	Max
Mass load	15	4.8	9.5	19
pH	5.9	0.4	5.3	7.0
OM	1578	364	17	1752
EC	169	96	10	298
Ca	874	191	190	1780
Fe	368	132	7.4	1426
Al	562	183	140	1832
Zn	21	6.2	0.1	43
Ti	127	45	0.6	304
Mn	112	39	0.4	58
Pb	4.8	3.5	Bdl	18
Ni	2.4	1.5	Bdl	30
Cr	1.9	1.2	Bdl	4.87
NO_3^-	757	404	74	1429
SO_4^{2-}	618	277	60	1335
NH_4^+	286	139	33	945
Na^+	59	74	6.5	366
$C2O_4^{2-}$	45	28	Bdl	130
Cl^-	30	54	15	245
Mg^{2+}	22	22	4.1	80
K^+	16	22	17	115
PO_4^{3-}	9.8	11	1.4	50
HCO_2^-	3.9	12	28	59
F^-	0.4	0.8	0.5	3.2
$CH_3O_3S^-$	0.4	1.8	Bdl	10
NO_2^-	0.1	0.4	1.2	2.2
$C_5H_{12}O_5$	8.9	12	Bdl	23
$C_6H_{14}O_6$	1.9	1.6	Bdl	7.7
$C_6H_{12}O_6$	20	30	Bdl	90

https://doi.org/10.5194/acp-2021-106
Preprint. Discussion started: 6 April 2021

Atmospheric Chemistry and Physics Discussions

1275 **Table 5.** Aerosol composition according to air mass

Aerosol Components	Air mass (μg/m^3)			
	NOA	ACE	MCE	SD
Mass load	19	30	23	54
Dust	96	12.6	11.7	44
Sea salt	0.6	0.7	0.3	0.3
OM	1.2	2.7	1.8	3.9
EC	0.2	0.7	0.3	0.2
NO_3^-	0.8	1.8	0.9	1.4
nss-SO_4^{2-}	0.6	1.9	0.8	1.7
NH_4^+	0.2	0.6	0.3	0.4
Water content	4.1	5.9	5.1	1.1
UM	2.1	2.9	2.5	1.2